ELSEVIER

International Journal of Mass Spectrometry 212 (2001) 413–443

International Journal of Mass Spectrometry

www.elsevier.com/locate/ijms

Gas-phase ion chemistry

The crossed-beam scattering method in studies of ion-molecule reaction dynamics

Zdenek Herman*

Joint Institute for Laboratory Astrophysics, University of Colorado, Boulder, CO 80309-0440

Received 11 April 2001; accepted 9 July 2001

Abstract

An overview of experimental techniques and instrumentation used in beam scattering studies of the dynamics of elementary ion-molecule reactions is presented. Procedure used in processing and presenting the scattering data is summarized. Selected examples of scattering studies are given to illustrate on some of the processes studied the achievements of this method in investigating ion-molecule dynamics, in particular the dynamics of chemical reactions of ions. (Int J Mass Spectrom 212 (2001) 413–443) © 2001 Elsevier Science B.V.

Keywords: Ion-molecule reaction dynamics; Ion scattering; Experimental methods; Data processing

1. Introduction

Over the past fifty years, studies of chemical reactions between ions and neutral molecules have developed into a large field of research in chemistry and physics. Systematic research of chemical processes between ions and neutral begins with the observation of the nonclassical ion CH_5^+ in collisions of methane cations with neutral methane molecules in the fifties [1,2]. For more than a decade the vehicle for studies of ion-molecule reactions was the ionization chamber of a mass spectrometer. Large amount of data on the nature of chemical products formed and on rates of ion-molecule processes was obtained during those years. In the early sixties, requirement for more detailed information on ion-molecule processes prompted the development of special instrumentation. It was in this period that several special techniques originated, in particular the swarm techniques (the flowing afterglow [3] and later on the selected-ion-flow-tube method [4]) for studies of reaction kinetics of thermal ions, the ion cyclotron resonance method [5] and its variations, and special instrumentation for beam studies of ion-molecule processes.

The beam techniques made it possible to study

* E-mail: zdenek.herman@jh-inst.cas.cz

JILA Visiting Fellow 2000-2001.

Permanent address: J. Heyrovský Institute of Physical Chemistry, Academy of Sciences of the Czech Republic, Dolejškova 3, CZ-182 23 Prague 8, Czech Republic

Dedicated to R. Graham Cooks on the occasion of his sixtieth birthday.

PII S1387-3806(01)00493-6

kinetics and dynamics of ion-molecule processes in the near-thermal and hyper-thermal collision energy range under single-collision conditions. The beam techniques are characterized by spatial separation of the site, where reactant ions are produced, where reactive collisions take place, and where product analysis is carried out. The development of the field, various instrumentation aspects and its achievements has been reviewed several times [6–12]. In principle, the beam techniques can be grouped into the following categories:

(a) Ion beam-collision cell techniques;
(b) Crossed-beam techniques;
(c) Merged-beam techniques;
(d) Guided-beam techniques.

The beam-collision cell (random gas) experiments provided large amount of valuable data especially in the early stages of the beam experiments and at higher collision energies, where the random orientation of the neutral reactant velocities did not play a significant role. At low collision energies this could represent a significant problem. Cooling of the reactant gas to decrease the thermal motion of the reactant gas was of a limited use only. The advantage of the collision cell was a relatively high intensity of the product ions, even under single-collision conditions.

The crossed-beam scattering technique largely diminished the shortcoming of the spread of relative collision energies of the beam-random neutral arrangements. It made good quality data on both angular and energy (velocity) distributions of the product ions accessible, and thus it turned out especially suitable for studies of the dynamics of ion-molecule collision processes. However, localizing the reaction zone to the crossing of the two beams (a volume typically of a few mm^3 at most) led to a considerable decrease of the product ion signal, and thus a drop of as much as 10^5 between the reactant ion and useful (scattered) product ion signal was not an exception. Determining absolute neutral reactant concentration is complicated and thus absolute total cross section measurements are difficult; this technique is the main subject of this contribution and details of this method will be discussed later.

The merged beam technique made it possible to achieve very low collision energies defined by the difference in velocities of two fast moving beams (relative kinetic energies 10-times lower than the thermal energy at ambient temperatures were reported). The technique requires that the fast neutral beam be prepared by charge exchange neutralization of an ion beam; this makes it possible to prepare, in principle, thermodynamically unstable neutral reactants like radicals. However, the internal state distribution, especially in case of molecular neutrals is usually not well defined as a result of the ionization-neutralization process in their preparation. Also, angular distribution information is practically lost with fast (keV) moving reactants in the laboratory frame of reference. The merged-beam technique provided valuable data in particular in measuring absolute total cross sections and their dependence on collision energies. The method belongs to more difficult and costly techniques applied to studies of ion-molecule collision processes. Critical appraisal of its advantages and shortcomings has been reviewed earlier [11].

The guided-beam technique, developed in the seventies by Teloy and Gerlich [13], uses multipole radio-frequency fields to guide or trap low energy ions. The guided-beam machines provide an excellent tool for reaching low collision energies and, in combination with either random-gas collision cells or crossed beams, an access to reliable measurements of total cross sections and their dependence on collision energy. They can also provide data the product velocity distributions along the beam axis and a possible application to obtain at least rough information on angular distributions has been described [12].

Experimental approach to fundamental questions concerning microscopic reaction mechanisms of ion-molecule processes has been connected mostly with beam-random gas collision cell and crossed beam scattering techniques. This paper is a review of the instrumentation used in these studies of ion-molecule reaction dynamics. Only approaches in which both angular and product translational energy data were obtained will be discussed. Some of the other approaches, complementing the beam reactive scattering

data on the dynamics (beam studies of reaction product chemiluminescence) will be briefly mentioned. Ion scattering studies encompass a much larger variety of elementary ion collision processes such as elastic scattering, inelastic scattering, dissociative scattering and collision-induced-dissociation (CID) processes, ion scattering of surfaces etc. Reviewing instrumentation used in studies of the dynamics of these ion-molecule collision processes would require a much more extensive article. Therefore, the scope of this contribution was limited to instrumentation used in studies of ion-molecule reaction dynamics, namely chemical reactions of ions, with only shorter references to other related collision processes (charge transfer processes, CID). Also, selected illustrations of the phenomena observed refer only to these areas.

2. Experimental techniques

The aim of studies of the dynamics of elementary chemical processes is elucidation of

(a) Collisional mechanism of the reaction;
(b) Influence of specific energy of the reactants on the course of the reaction;
(c) Partitioning of available energy between the products.

One way to achieve these goals is to investigate the elementary processes under single-collision conditions in scattering experiments. The answer to (a) is largely connected with the angular part of the problem. The overall energy balance of a single-collision event is given by

$$E_{TOT} = T + V + R + (-\Delta H_R) = T' + V' + R' \quad (1)$$

In Eq. (1), T is the relative translational energy of the reactants, V and R their vibrational and rotational energy, $(-\Delta H_R)$ the reaction heat, primed terms refer to the products; electronic energy is usually included into the $(-\Delta H_R)$ term. The relative translational energy of the reactants, T, can be rather well controlled in ion-molecule studies over a wide range of energies from quasithermal to highly hyper-thermal. Various methods can be used to control the internal energy of the reactants or keep it small with respect to T. By measuring the translational energy distribution of the products one can at least obtain information on product energy partitioning between the external and internal degrees of freedom. In high-resolution studies, information on V' and R' can be obtained from structures in product translational energy distribution. Otherwise, this information can be obtained from complementary spectroscopic studies (e.g. investigation of product luminescence).

The development of crossed beam scattering studies of ion-molecule reactions has been closely connected with the development of beam studies of neutral-neutral chemical reactions under single-collision conditions in the sixties. The idea of the experiment was simple: prepare both reactants, a mass-selected ion and a neutral, in the form of beams of defined velocity distributions, let them collide in a reaction zone under a defined angle, and measure the velocity and angular distribution of the product ion of this elementary chemical act under single collision conditions.

An ideal beam scattering experiment is schematically shown in Fig. 1. The ions are formed in an ion source and possibly state-selected there; they are then subjected to mass selection of the reactant ion species, deceleration and velocity (energy) selection. Similarly, the neutral reactant beam is prepared in a neutral beam source and velocity and internal state analysis is applied to it. The two beam cross in the scattering center. The detector behind the detection slit analyzes the scattering angle, velocity (energy) distribution, mass, and possibly internal state of the ion product formed. Analogously, angle, velocity and internal state analysis can be (and sometimes was) applied to the neutral products.

The instrumentation actually used approaches this ideal configuration to a varying degree. Usually, the analysis of the ion product (or neutral product) internal state was carried out in special independent experiments (chemiluminescence of reaction products [14]), while in the beam scattering experiments the emphasis was on determination of angular and velocity (translational energy) distributions of the product

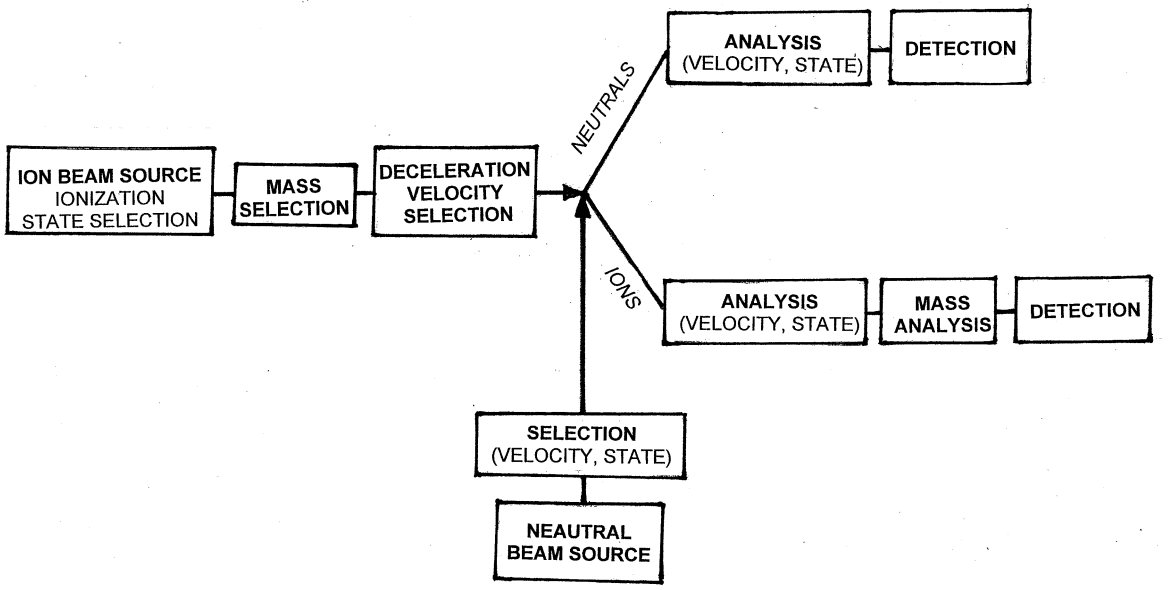

Fig. 1. Schematics of an ideal crossed-beam scattering experiment.

ions. The following sections review the variety of procedures used to achieve this goal.

2.1. Ion sources

Crossed-beam experiments require rather high-intensity reactant ion beams with a small energy spread and well-characterized internal energy distributions. The first requirement made electron impact ionization, a method well developed for mass spectrometer ion sources, the most likely candidate for ion beam production. Various variations of electron impact ion sources (Nier-type source with a collimated crossed electron beam [15], oscillating electron beam [16]) were used. The sources often offered reasonable ion beam energy spreads of about 0.2 eV, full-width-at-half-maximum (FWHM) [15] so that no further energy selection was necessary. The Colutron ion source, basically a discharge source [17], was often successfully used for reactant ion beam production: because the mean electron energy in this type of source is generally lower than in conventional electron impact sources, preferential formation of ions in the ground state (in comparison with higher-lying excited states) was reported as one of its it's advantages [17]. Use of photoionization [18] or multiphoton ionization [19] to produce reactant ion beams has been exceptional and directed to total cross section measurements with state-selected reactants rather than to scattering experiments.

Electron impact ionization gives rise to both ground state and electronically excited states. For molecular ions, the vibrational state population is determined by the Franck–Condon overlap between the neutral molecule and molecular ion states. This may either lead either to the formation of the ion prevailingly in its ground vibrational state (e.g. $C_2H_2^+$) or to an inconveniently large internal excitation of the molecular ion formed (e.g. H_2^+, CH_4^+, $C_2H_4^+$). In addition, electronically excited states of molecular ions may decay in radiative transitions to the ground state and thus further modify the initial population of the vibrational states before the reactant beam reaches the collision zone. The initial internal state population of molecular ions can be roughly estimated [20] as a product of the energy dependence of the population of the ion in the break-down pattern and the population of internally excited states in the photoelectron spectrum

of the molecule (assuming that the impact of fast electrons, $E_{el} > 100$ eV, leads to similar results as photon impact and that autoionization may be neglected).

Collisional relaxation or an ion-molecule reaction in an electron impact ion source at elevated source pressures has been successfully used to modify the inconvenient internal energy content of the reactant ion beam. Thus, e.g. $F^+(^1D)$ excited state could be quenched by addition of NO into the ion source [21], internally relaxed H_3^+ and ArH^+ were prepared by in Ar-H_2 mixtures at elevated source pressures [22], pure $N^+(^3P)$ ground state beam was formed in a mixture of nitrogen with an excess of He [23] [the main process is charge transfer between He^+ and N_2 leading to the dissociative $N_2^+(C)$ state giving $N^+(^3P)$], a hydrogen ion beam preferentially with $H_2^+(v=0,1)$ was prepared in a mixture of H_2 with an excess of Ne at a source pressure of about 10^{-3} mbar [24] (chemical reaction with Ne in the ion source, leading to NeH^+ removed $H_2^+(v \geq 2)$ formed by electron impact).

An innovative method of relaxing reactant ions was the use of rf trapping in storage ion sources [12,13]. Ion formed by electron impact could be accumulated in U-shaped or labyrinth-shaped electrodes by rf fields to relax by long storage or by collisions and reactions with added gases to produce intense short pulses (see also Sec. 3.3.).

2.2. Ion beam preparation

For mass selection of the ion beam, magnetic sector instruments have been most often used [15,16,25–29]. Also, the use of a Wien filter for mass analysis has been reported [30]. This requires in most cases acceleration of the ions, extracted from the ion source, to at least a few hundred eV and their subsequent deceleration and focusation. In several instances quadrupole mass filters, operating at input ion energies of a few eV, were used [31,32]. Subsequent focusation and collimation of the outgoing ion beam was then employed. For the deceleration of mass selected ion, multi-element deceleration lenses of various types have been described. The improved Lindholm-type multielement lens [15] with several deceleration-reacceleration stages has been used in several devices [14,25,32]. Also, an exponential lens, specially constructed for ion-molecule collision studies [28], has been successfully employed [27,28]. Quadrupole lenses, einzel-lenses and immersion lenses were applied to focus and control the ion beams.

As mentioned earlier, in cases where the energy spread of the ion beam from the source was about 0.2–0.3 eV, no further energy analysis was employed, as this spread was sufficient for the purpose in question. However, several devices used energy analysis to prepare ion beams of very low energy spread below 100 meV (FWHM) [29–31]. For this energy analysis, both cylindrical [29] and hemispherical [30,31] energy analyzers have been used. Energy spreads as low as 30 meV have been reported [30] for beams used in high-resolution ion-molecule collision studies.

2.3. Neutral beam preparation

Effusive beam sources were almost exclusively used in the improved version of multichannel arrays to improve the intensity of the neutral beam along the beam direction. Small distance from the scattering center and use of a collimation slit resulted in well-characterized neutral beams [15] of angular spreads of less than 10° (FWHM) which found standard use in studies of the dynamics of ion-molecule reactions [15,33]. The velocity distribution in these beams is Maxwellian and the population of internal states determined by the temperature of the source. Equivalent number densities obtained with these beams were of the order of 10^{12}–10^{13} cm^{-3}. Chopping of the neutral beam and lock-in detection of the scattered ion signal was an effective way to deal with the background scattering problems. Effusive beam were sometimes cooled to lower the velocities of the neutrals [31].

A considerable improvement of the neutral beam quality came with the use of supersonic and seeded beams [27,28]. Gas at a high-pressure and stagnation temperature expands through a small pinhole into vacuum and passes through a conical skimmer to form a supersonic beam. The expansion conditions at sufficiently high Mach numbers, lead to an increase of

the most probable velocity of the beam particles and to a considerable narrowing of their velocity distribution, in comparison with effusive beams. At the same time, the temperature of the internal degrees of freedom of the expanding particles is reduced to a few K. The use of supersonic beam sources greatly increases requirements on the pumping speed, and thus multiple differential pumped arrangements have to be used.

2.4 Product analysis

Angular analysis was mostly performed by rotating the two beams about the collision center with respect to the fixed detection slit of the detector or by rotating the detection-slit-detector system about the intersection of two fixed beams. Extracting the angular information from varying the guiding field potential and determining the transverse product ion velocity component in guided beam devices [12] may provide an entirely new approach to measurement of angular distributions. The use of position sensitive detectors in ion-molecule studies has been so far limited [34,35].

For product ion energy analysis the simple stopping potential analyzers, consisting of two parallel high-transparency grids perpendicular to the path of ions, have been used [15,25,33]. Their advantage is in an easy measurement of the total product intensity at a particular scattering angle and in attaining full collection efficiency, if effective focusation and acceleration the transmitted ions was applied [15,33]. Considerable drawback is in resolving fine structure in the stopping potential curves and in measuring small contributions of low energy ions against much larger contributions of high-energy ions. Electrostatic deflection analyzers, cylindrical [24,27,29] or hemispherical [15,26,30] overcome the latter shortcoming. Difficulties with changing collection efficiency for ions of different energies can be overcome by acceleration/deceleration of the incoming ions and operating the analyzer at fixed throughput energy, the technique perfected in electron energy analysis. Time-of-flight analysis on angle-selected ions guided in multipoles [11,12] is without doubt an efficient method of product ion velocity analysis.

For mass analysis of the products ions both magnetic and quadrupole mass spectrometer systems have been used the latter being much more convenient in rotatable detectors.

2.5. Product detectors

The problem of ion detection in scattering experiment is to determine extremely small ion signals of product ions as well as monitoring orders of magnitude larger signals of the reactant ions. In all instruments multipliers have been used. Open diode multipliers have been often used or channeltron multipliers in the counting mode applied to detect individual charged products. A reliable detection system applied rather often is the Daly detector [36]: positive ions are accelerated toward a metal surface by a high potential difference (30 keV), where they eject secondary electrons; these are in turn accelerated by the same potential towards a scintillator plate, the photons formed are amplified by a photomultiplier (placed outside of the vacuum part), and counted as individual events. The use of position-sensitive detectors [34,35] and channel plates seems to open a new chapter of detectors for scattering experiments.

Detection of neutral particles has been limited so far to fast neutral products of ion-molecule reactions on a channelplate position-sensitive detector [33,34] and to a rather unexpected detection of neutral H-atoms (energies less than 100 eV) from charge transfer collisions between protons and molecules [28] on an open dynode multiplier. The detection efficiency for these neutral particles is much lower than for ions, but the very fact that neutral products from ion-molecule collisions could be detected considerably broadened information on ion-molecule dynamics. In product chemiluminescence experiments spectra of both ion and neutral products were measured.

Chopping or modulating the neutral beam and detecting the modulated product ion signal using the lock-in techniques has been used in several crossed-beam machines to detect the signal originating in the tiny beam intersection from the, usually much larger,

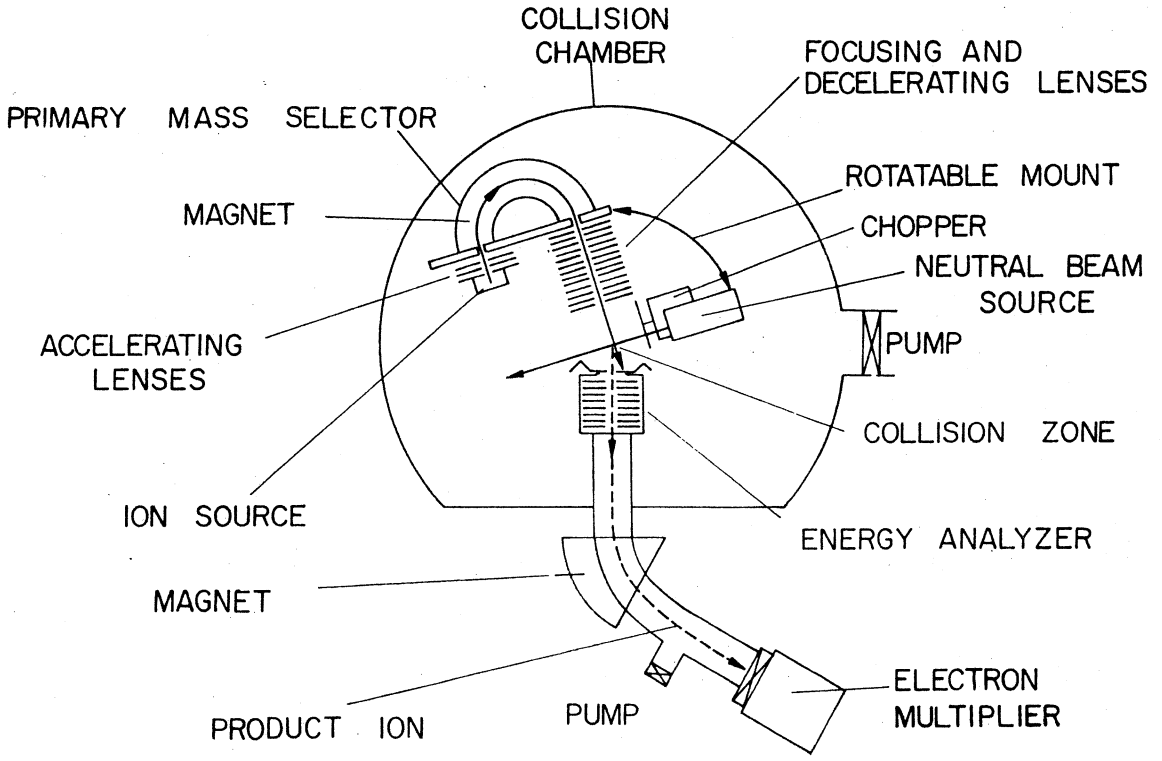

Fig. 2. Schematics of the crossed beam scattering apparatus EVA I [15].

signal from the reaction with background molecules [15,27,33].

3. Survey of beam and crossed-beam instruments used

The first experiment in which laboratory angular distribution of a product of an ion-molecule reaction (N_2D^+ formed in $N_2^+ + D_2$ collisions) was measured [37] showed that measuring only the angular distribution did not provide sufficient information to decide unambiguously on the dynamics of the process. This is because in most cases the large hyper-thermal velocity of the ion reactant leads to confining the angular scattering to a rather narrow cone along the reactant laboratory velocity. On the other hand, early simple measurements of the product ion laboratory energy along the reactant ion beam direction enabled a good insight into the kinematics and provided the first data on direct stripping processes [38]. Thus it became soon clear that the combination of both these measurements was needed to obtain more detailed information on the dynamics of ion-molecule processes.

3.1. Crossed-beam apparatus EVA I

The Yale instrument EVA I (R. Wolfgang's group, 1966 [15]) was one of the early instruments which used crossed beams and provided scattering data on a series of ion-molecule reactions of various types [6,15,39]. It consisted (Fig. 2) of a reactant ion beam source, a collimated multichannel jet neutral beam source, a stopping potential energy analyzer, and a detection mass spectrometer. The two-reactant beams crossed at right angles and could be rotated about the scattering center for angular distributions measurements. The ion beam source consisted of an electron

impact ion source from which ions were extracted, accelerated to 100–300 eV, mass selected by a 180° permanent magnet mass analyzer, and decelerated in a modified multielement Lindholm-type lens. Reactant ion beams (dimensions 0.4×1.0 mm^2) of laboratory energies down to about 0.5 eV could be obtained; the beams have energy spreads of about 0.15–0.3 eV (FWHM) and angular spreads of about 1–1.5° (FWHM). The intensity of the ion beams was close to the space-charge limit (e.g. about 1×10^{-10} A at the laboratory energy of 1.5 eV) and the angular spread was consistent with the expected space-charge broadening of the beam. The neutral beam was typically collimated to an angular spread of 10° (FWHM). The neutral beam was chopped by a rotating slit and the product ions were detected by a lock-in amplifier and tuned to the chopping frequency to remove the effects of background scattering. The reactant and product ions passed then through a detection slit to a simple stopping potential analyzer (two parallel fine grids) and they were then focused and accelerated into the detection mass spectrometer (a 60° magnetic instrument, differentially pumped). The ion currents were detected on a dynode multiplier. The measurements consisted of determining laboratory angular distributions and profiles of energy distribution of the product ions at a series of scattering angles. These original data were then used to construct contour scattering diagrams of the product ions.

An improved, larger variation of this type of instrument (EVA II, [33]) has been used successfully in Prague for a variety of studies of the dynamics of chemical reactions of cations, charge transfer processes, collision induced dissociation of polyatomic ions [40], charge transfer processes and chemical reactions of dications, and, more recently in a modified version, for ion-surface scattering studies [41].

3.2. Single-beam instruments

Several ion beam-scattering chamber instruments were built which provided both angular and product translational energy distribution data.

In the Berkeley instrument (B. Mahan's group, 1967 [16]) ions were formed by electron impact in a source with an axially oscillating electron beam, extracted, accelerated, and focused by a quadrupole lens into a magnetic momentum analyzer; mass selected ions were decelerated or accelerated and focused into the collision cell (two concentric cylinders with apertures). Ions leaving the collision cell passed through a 90° electrostatic analyzer and were then focused into a quadrupole mass filter. The detector consisted of an aluminum plate at 25 keV from which accelerated ions released secondary electrons, which were then accelerated and counted on a semiconductor detector. The reactant ion beam had an energy spread better than about 0.75 eV (FWHM) and angular resolution of the detector train was 2.5°. The instrument produced large amount of data on ion-molecule processes, namely at higher (>25 eV) reactant beam energies.

The single-beam device at Gainesville (T.L. Bailey's group, 1966 [25]) also produced ions by electron impact. The ions were extracted and accelerated to 200 eV into a 60° magnetic mass analyzer; emerging ions were decelerated, focused by a quadrupole lens, and subjected to energy selection in a 127° cylindrical analyzer before entering a collision cell. Product ion leaving the collision cell were collimated and directed into the second cylindrical energy analyzer (analogous to the first one) and mass analyzed by a quadrupole spectrometer. Counting of the multiplier output pulses was used to measure the product ions. The detector train could be rotated about the collision cell between −10° and +85°. Ion beams from 2.5 eV up of energy spreads of 0.3 eV (FWMH) or higher could be used.

The Berlin instrument (A. Henglein's group, 1971 [26]) used electron impact ionization, 180° magnetic mass analyzer, a multielement deceleration lens similar to the one mentioned above [15], a collision cell, a stopping potential product ion energy analyzer, and a quadrupole mass analyzer. Product ions were counted using a channeltron. For angular distribution measurements, the reactant ion beam source could be rotated about the collision cell.

In the Baltimore apparatus (W.S. Koski's group, 1976 [31], Fig. 3) ions were produced by electron impact, mass analyzed by a quadrupole mass spec-

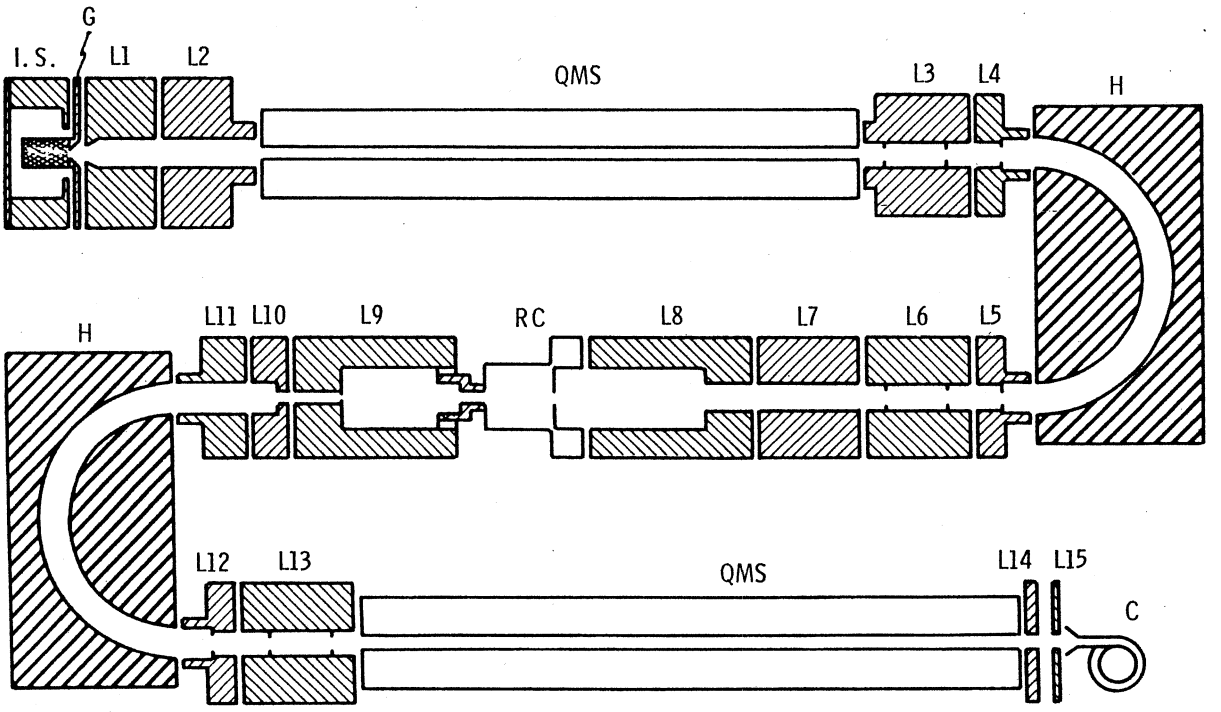

Fig. 3. Schematic diagram of the Baltimore single-beam apparatus [31]: I.S.-ion source; L1–L13 - lens elements; QMS - quadrupole mass spectrometers; RC -reaction cell; H - hemispherical energy analyzers; C - channeltron multiplier.

trometer, energy selected by a 180° spherical analyzer, and focused into the collision cell. The ions leaving the collision cell entered the detector, which consisted of another 180° spherical energy analyzer and a quadrupole mass analyzer followed by channeltron particle multiplier. The detector could be rotated about the collision cell and both angular and kinetics energy data could be obtained. The use of spherical energy analyzers made it possible to obtain reactant ion beams of energy spread 100 meV (FWHM) and vibrational structure in translational energy distributions of products f some reactions could be partly resolved. The instrument was successfully used in a series of studies of atomic, diatomic ions and simple polyatomic ions with hydrogen.

3.3. Freiburg differential scattering apparatus

The crossed-beam scattering apparatus built in Freiburg in the seventies (Gerlich [12,32]) was innovative in using rf devices for the differential scattering measurements (Fig. 4). Reactant ions were prepared in a U-shaped storage source by electron impact and they could relax before being extracted as a microsecond ion pulse, which was energy and mass selected in a quadrupole, focused and collimated before reaching the scattering center. The beam divergence was limited to 1° and ion beam energies down to about 0.2 eV could be obtained. The neutral reactant beam was introduced perpendicularly through an effusive gas inlet, which could be cooled to 80 K to reduce the velocity spread of the molecules in beam. The two beams could be rotated about the collision center between −20° and +70°. A collimator restricted the angular acceptance of the detector to 3°. The product ion pulse was velocity analyzed by the time-of-flight method in a 100 cm long hexapole beam guide. It was then accelerated to 3 keV, mass analyzed by a magnetic sector spectrometer, and detected with the use of a Daly-type system. Detailed differential scat-

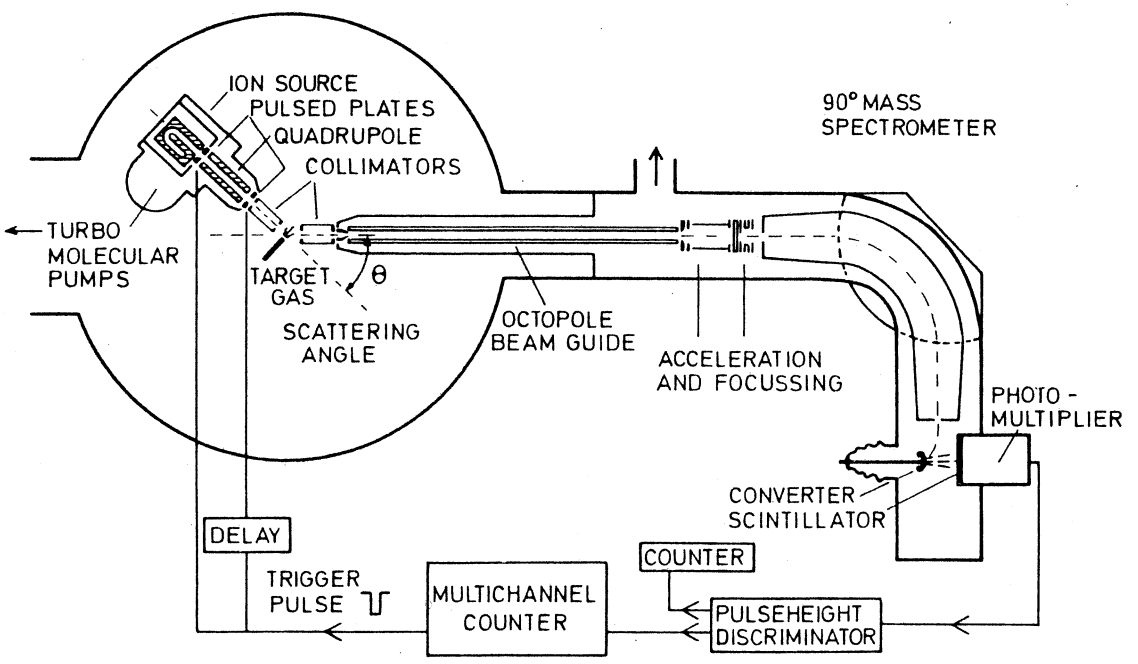

Fig. 4. Schematics of the Freiburg differential scattering machine (adapted from [32]).

tering data were obtained for the proton-deuteron exchange reaction in the H^+-D_2 system in which rovibrational structure of molecular product (HD) states could be partially resolved in the product ion D^+ velocity spectra [12,32].

3.4. Kaiserslautern crossed-beam instrument

The crossed-beam instrument constructed at Kaiserslautern (F. Linder's group, 1978 [30]) was a high-resolution apparatus used in a variety of ion-molecule scattering studies, notably in studying the $H^- + D_2$ exchange reaction in which population of vibrational states of the molecular product were resolved in product ion velocity spectra.

Reactant ions were formed and mass selected in a side arm of the machine and introduced into the main chamber at energy of about 200 eV. There they were decelerated to 3 eV and injected into an electrostatic energy selector consisting of two 127° cylindrical condensers in series. The reactant ion beam had a very small energy spread (30 meV FWHM) and a small angular divergence (±0.5°). A skimmed supersonic nozzle beam had an angular divergence of ±1.5° and it was directed vertically into a big pump. The detector system, of a similar configuration as the reactant beam energy selector (two 127° cylindrical analyzers), could be rotated in the plane perpendicular to the plane of the two beams. Ions emerging from the analyzer were directed into a multiplier, without mass selection. The overall angular resolution of the apparatus was about ±1°.

3.5. Rochester crossed-beam apparatus

The efficient instrument at the University of Rochester (J.M. Farrar's group, 1980 [27]) was designed with a special care for defining the neutral beam. Reactant ions (Fig. 5) were produced in an electron impact ion source, which could be operated at elevated pressures to use quenching gases. Ions were extracted, accelerated, focused by quadrupole lenses into a magnetic sector mass analyzer, and decelerated in a multielement exponential retarder. The neutral reactant beam emerged from a supersonic beam source, which could be seeded with a carrier gas to

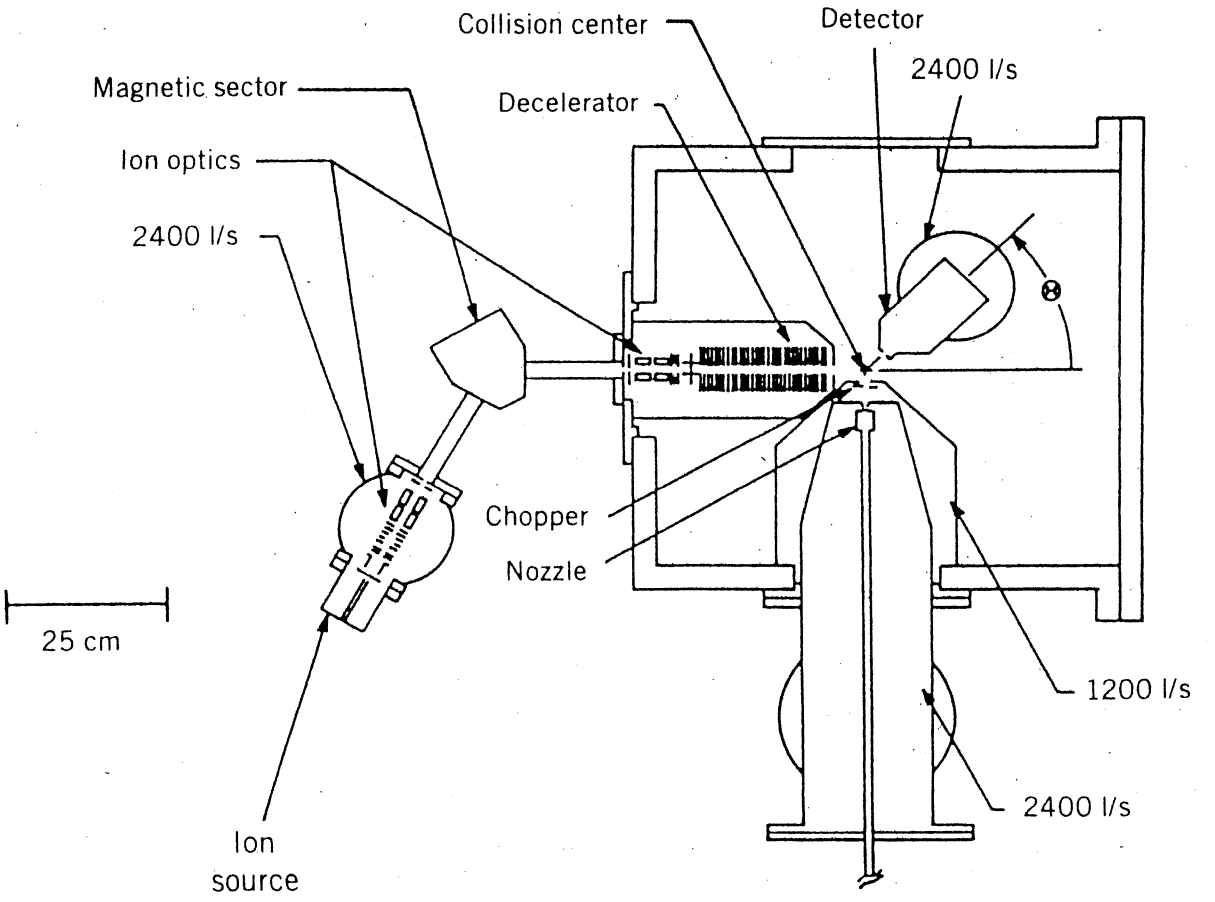

Fig. 5. Schematics of the Rochester crossed-beam scattering apparatus [27].

accelerate the reactant neutral species and facilitate the kinematics analysis; after passing through a skimmer, the beam was chopped and collimated by a slit to the angular width of 2° (FWHM). The product detection system, rotatable in the plane of the two beams, consisted of an electrostatic 90° spherical energy analyzer and a quadrupole mass spectrometer equipped with a scintillation counter. The geometric angular resolution of the apparatus was ~2.1° (FWHM) and the energy resolution of the energy analyzer 75–150 meV. A series of fine studies was carried out with this instrument, among others on the kinematically difficult reactions between H_2^+ and rare atoms or simple diatomics, reactions involving metal ions, and more recently in beautiful studies of anion-neutral reactions (see Sec.5.4.).

3.6. Salt Lake City instrument

The special feature of the crossed-beam apparatus built at the University of Utah (J.H. Futrell's group, 1977 [28]) was a high-pressure chemical ionization source enabling at least partial relaxation of the ions formed by electron impact. Laboratory energies of the ion beam of less than 1 eV could be obtained of energy spreads of about 0.3 eV (FWHM). A 60° magnetic analyzer and a novel exponential deceleration lens were used to form the ion reactant beam. An intense (equivalent density at the crossing point of 10^{-5} Torr) neutral reactant was produced in a supersonic nozzle and had an angular spread of 4°. The rotatable detector consisted of a 90° cylindrical energy analyzer, a quadrupole mass analyzer, and an

electron multiplier detector. The apparatus was successfully used in a series of studies of the reaction dynamics of chemical reactions and charge transfer processes.

3.7. Newark CID scattering apparatus

The apparatus designed especially for studies of collision-induced dissociations, with both energy and angular analysis of the ion products, was constructed at the University of Delaware (J.H. Futrell's group, 1988 [42]). It is a hybrid tandem mass spectrometer with a VG double-focusing mass spectrometer as the ion beam source; the ions, mass analyzed at 3 keV, can be decelerated to ensure operation range between less than 1 eV and 3 keV. The neutral beam source is a collimated supersonic nozzle arrangement crossing vertically the reactant ion beam. The product ion analyzer consists of an energy analyzer (a hemispherical deflection system of a novel type), a quadrupole mass filter, and an electron multiplier. Angular distributions are obtained by rotating the analyzer about the collision center. The energy spread of the reactant beam is about 3–4 eV (FWHM) for ion energies up to 100 eV, the angular resolution is about 3°.

3.8. Göttingen inelastic scattering apparatus

The high-resolution instrument, constructed in Toennies's group in Göttingen (1986 [29]) was originally designed for studies of proton-molecule inelastic energy loss studies. However, it turned out during these studies that the detector was able to pick up signals of fast neutral H-atoms formed in charge exchange collisions with the target molecules. The machine could be thus also used to provide data on charge transfer processes. The instrument produced protons in a Colutron source. After mass analysis and fine energy analysis in a 127° selector, the ion beam was pulsed and focused onto a unskimmed crossed beam of target molecules; the energy-loss analysis was carried out using time-of-flight analysis in a long flight tube. When inelastically scattered ions were blocked off by a repeller field, neutral H-atoms of energies below 100 eV could be detected on the first dynode of the Be-Cu electron multiplier with an efficiency of about 1% of that for H^+. Very high resolution of the machine (better than 100 meV) made it possible to obtain unique data on charge transfer between protons and molecules with vibrationally resolved structure of the charge transfer molecular product.

3.9. Orsay coincidence instrument

The Orsay instrument (1985 [34,35]) was a novel type of machine, employing techniques not used before, like detecting products in coincidence on a position-sensitive detector. It operated on the principle of extracting information from the coincidence of two reaction products (ion and fast neutral) formed in collisions in crossed beams (Fig. 6). It was used in a series of important experiments to study dynamics of chemical reactions between atomic anions X^- (Cl^-, Br^-, S^-) and hydrogen at higher collision energies in which a variety of charged and neutral products was measured. The ions were produced in a discharge source and focused by an einzel-lens into the crossing with a narrow supersonic beam of H_2. Negative species (e^-, H^-) formed in the collisions were extracted perpendicularly by a small extraction field, applied to two parallel grids, accelerated and detected on a multichannel plate device. The fast-scattered neutral particles were collected on a position-sensitive detector (a double-chevron multichannel plate with 16 anodes). The overall angular resolution of the device was $\pm 3°$. The multicoincidence method consisted in simultaneous time and spatial correlation between the slow charged particles (e^-, H^-) and neutral fast particles (HX, X).

3.10. Product chemiluminescence apparatus

Measurements of luminescence of products of ion-molecule collisions has been important complementary information to beam scattering studies in ion-molecule reaction dynamics, whenever emission from electronically excited product states could be detected. From the recorded spectra, data on the population of electronic, vibrational, and rotational

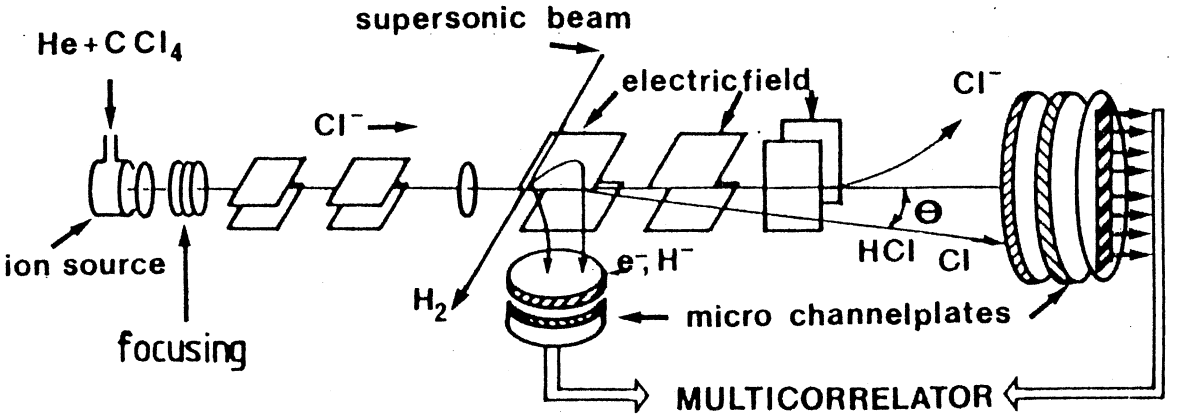

Fig. 6. Schematic view of the Orsay coincidence Instrument [34].

states of the products could be obtained, very important information on internal degrees of freedom of the products to complete the picture of state-to-state reaction dynamics. The machine built and operated for many years successfully in Göttingen (Ottinger, 1973 [14]) can serve as a typical example of this type of instrumentation. (Fig. 7). Ions were produced in a Colutron-type discharge source, extracted, focused and accelerated to 1 keV into a 60° magnetic mass selector. The selected ions were then decelerated prior to entering the collision chamber by a simple immersion lens to energies from about 1 eV up. The central part of the collision chamber was viewed by an optical spectrometer. Emission from the chamber, emerging

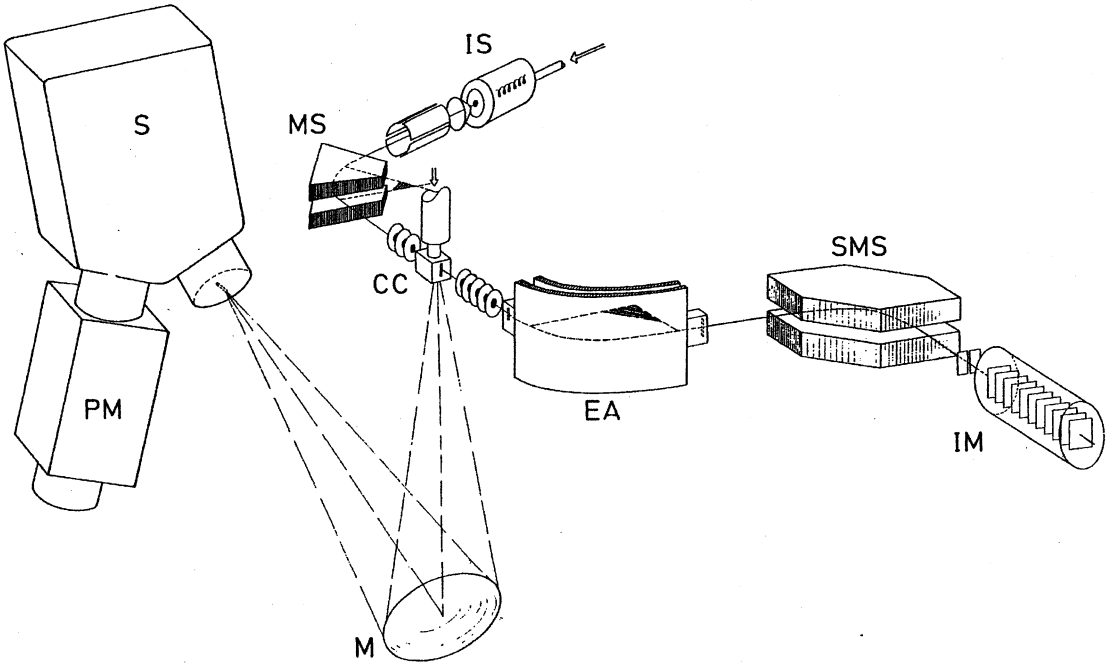

Fig. 7. Schematic diagram of the Göttingen chemiluminescence apparatus [14].

through a MgF_2 window at its bottom, was reflected by a concave Al mirror onto the entrance slit of a evacuable monochromator of a dispersion of 13.3 A/mm. Using different slit widths, optical resolution could be varied between 2 and 26 A (FWHM). A thermoelectrically cooled photomultiplier served as a detector. Attenuated beam of reactant ions and forward scattered product ions leaving the collision cell could be monitored by an energy analyzer-mass spectrometer-multiplier train.

3.11. Guided beam techniques

The principle of guiding ions in rf octupole fields has a long history and a very wide range of applications. The principle was used by Teloy to build an apparatus for measurements of collision energy dependence of total cross sections of ion-molecule reactions [13]. It consisted of an electron trap ion source, a magnetic mass spectrometer and an octupole ion guide (a version of the machine for differential scattering measurements, see Sec. 3.3.). Thereafter this first device was developed by Gerlich [12] into a universal guided beam apparatus. Various versions of this instrument have found a wide range of applications in ion beam studies and total cross section measurements [12].

The universal apparatus [12] consists of a rf storage ion source in which ions are formed by electron impact, trapped, and their internal energy thermalized. By opening the ion gate, an intense pulse of ions (few microseconds long) is sent into a focusing and mass selecting quadrupole and thereafter into a lens system. Another pulse applied to a gate in the lens systems provides additional time-of-flight velocity selection. The ions are the injected into an octupole via a funnel electrode. The octupole can be divided into several sections and its' central part is usually surrounded by a collision chamber, where collision processes may take place. Using a collision chamber at the end of the first octupole section and a fairly long second octupole section, time-of-flight analysis can provide velocity distributions of both the reactant and product ions along the direction of the octupole axis. The ions are then mass analyzed in a magnetic or quadrupole mass analyzer and detected using a multiplier.

The important feature of this technique is that reactant ion energies down to tens of meV can be obtained and, with various modifications of the collision cell arrangement, total cross sections even at these very low collision energies can be reliably measured. The reason why we mention this instrumentation in connection with scattering experiments is that it can also provide, in a relatively easy way, reliable time-of-flight data on velocity distributions of product ions along the direction of the reactant ion beam, with a high sensitivity and in the very low collision energy region, not readily accessible for beam scattering methods. Angular measurements were not included into the original design, but it has been shown recently [12] that by varying the guided beam potential, data on the transverse velocity component of the ions can be obtained and from it information on the angular distribution of the product ions formed can be derived.

4. Processing of scattering data: Newton diagram, scattering diagrams, and derived quantities

4.1. Basic assumptions of the classical treatment

The main task of the scattering method is deducing the asymptotic behavior of products from the asymptotic behavior of reactants, i.e. far from the collision center so that no interaction between them takes place. If molecular particles interact with each other randomly, i.e. regardless of their mutual orientation, the molecular species may be replaced by mass points to obtain a classical description of the state of the system in external (translational) degrees of freedom. This approach makes it possible to accept from the classical two-body collision theory general conclusions valid for the dynamics of elementary chemical processes, too. In the asymptotic regions the velocities of the particles are uniform and thus the dynamical state of the system can be described in the external degrees of freedom before and after the collision by

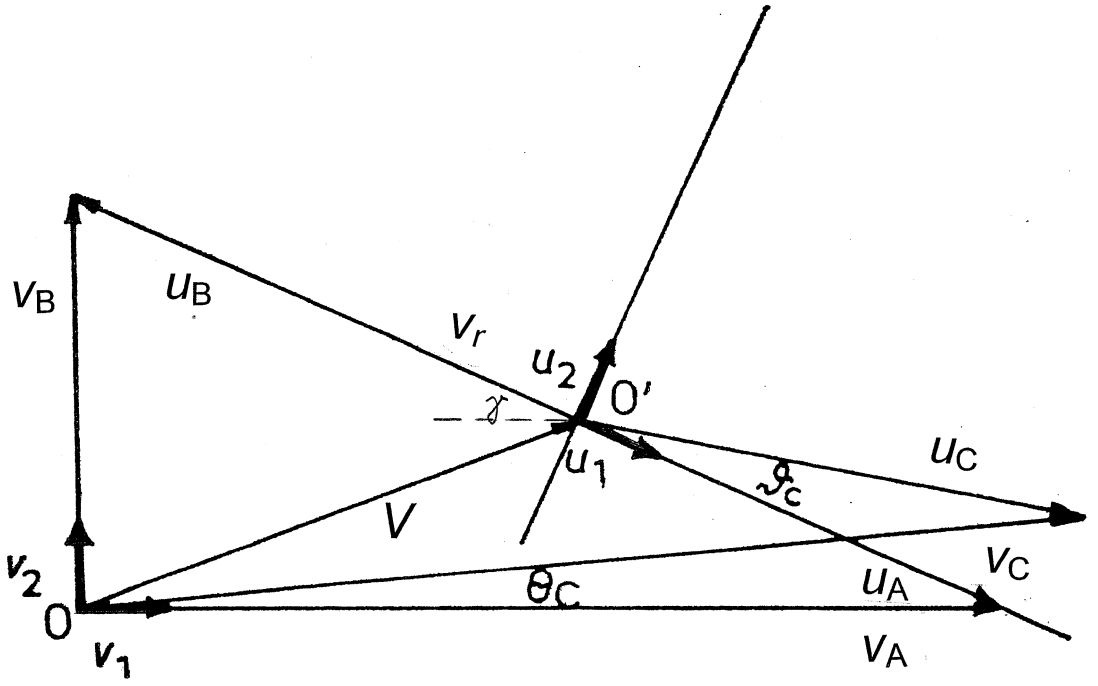

Fig. 8. Newton velocity vector diagram for a reaction A + B→ C + D showing the relations between the LAB and CM quantities. For more details see the text.

means of time-independent velocities of the particles, representing them by points in the velocity space of the system. The internal force acting on the system is a central force, the angular momentum of the system is a constant of motion, and the process is confined to a plane. Therefore, for the purpose of derivation of basic relations between the velocities, one may work only with a two-dimensional subspace of the velocity space (disregarding here the finite size of the beams). An extension of the following to three dimensions can be readily accomplished.

4.2. Newton diagram

Results of scattering studies on the dynamics of chemical reactions have been presented since the beginning in the framework of the Newton velocity vector diagram [43]. The Newton diagram provides a useful graphical representation of the velocity relation in the laboratory coordinate system (LAB), in which the experiment is carried out, and the center-of-mass coordinate system (CM), in which the analysis of the dynamics is conveniently made. The Newton diagram for a general reaction A + B → C + D is shown in Fig. 8 [44].

An orthogonal coordinate system can be defined in the (temporarily accepted) two-dimensional velocity subspace $\{O;\mathbf{v_1},\mathbf{v_2}\}$ of the origin O and unit base vectors $\mathbf{v_1}$, $\mathbf{v_2}$ (bold letters designate vectors). The system will be referred to as laboratory coordinate system (LAB). In general, the velocity vectors of the reactants A, B (of masses m_A, m_B and the total mass $M = m_A + m_B$), $\mathbf{v_A}$, $\mathbf{v_B}$ can be located at the origin O and represented as radius vectors, defined in the LAB system by expansions

$$\mathbf{v}_A = \sum_{i=1}^{2} \nu_{Ai}\mathbf{v}_i \tag{2a}$$

$$\mathbf{v}_B = \sum_{i=1}^{2} \nu_{Bi}\mathbf{v}_i \tag{2b}$$

where v_{Ai} and v_{Bi} (i=1,2) are Cartesian coordinates of the radius vectors in LAB and $\mathbf{v_i}$ are the unit base vectors. The relative velocity vector $\mathbf{v_r}$ of the reactants A, B is defined as

$$\mathbf{v}_r = \mathbf{v}_A - \mathbf{v}_B \tag{3}$$

and its norm is v_r.

In most experimental arrangements the beams intersect under a fixed angle of 90°. The LAB radius vectors of the velocities $\mathbf{v_A}$,$\mathbf{v_B}$ of the reactants A, B can be then oriented parallel to the unit base vectors $\mathbf{v_1}$, $\mathbf{v_2}$. Location of the vectors $\mathbf{v_A}$, $\mathbf{v_B}$ to O leads to representation of $\mathbf{v_A}$, $\mathbf{v_B}$ as radius vectors of the velocities the particles A, B would have if no interaction during the collision occurred (Fig. 8).

One can now construct another orthogonal coordinate system $\{O'; \mathbf{u_1},\mathbf{u_2}\}$ of the origin O' and the unit base vectors $\mathbf{u_1}$, $\mathbf{u_2}$. The expansion of the vector $\mathbf{V} = OO'$ in the LAB has the form

$$V = \sum_{i=1}^{2} V_i \mathbf{v}_i \tag{4}$$

Coordinates V_i and the angle of rotation γ of the new coordinate system are defined with respect to LAB in general by

$$V_i = (m_A v_{Ai} + m_B v_{Bi})\, M^{-1} \tag{5}$$

and

$$\gamma = \arccos[(v_{Ai} - v_{Bi})\, {v_r}^{-1}] \tag{6}$$

The origin O' of the new coordinate system $\{O'; \mathbf{u_1}, \mathbf{u_2}\}$ will then coincide with the point representing the LAB velocity of the center of mass of the reactants A and B and the unit base vector $\mathbf{u_1}$ will be parallel with the reactant velocity vector $\mathbf{v_r}$. The new coordinate system thus defined will be referred to as the center-of-mass system (CM). Analogous relations for $\mathbf{u_A}$, $\mathbf{u_B}$, and $\mathbf{u_r}$ (CM) apply as for $\mathbf{v_A}$,$\mathbf{v_B}$, and $\mathbf{v_r}$ (LAB):

$$\mathbf{u_A} = \sum_{i=1}^{2} u_{Ai} \mathbf{u}_i \tag{7a}$$

$$\mathbf{u_B} = \sum_{i=1}^{2} u_{Bi} \mathbf{u}_i \tag{7b}$$

and the relative velocity vector in the CM system

$$\mathbf{u}_r = \mathbf{u}_A - \mathbf{u}_B. \tag{8}$$

Transformation of the Cartesian coordinates of velocities corresponding to the transformation of the coordinate systems leads to

$$u_A = (m_B/M)\, v_r \tag{9a}$$

$$u_B = -(m_A/M)\, v_r. \tag{9b}$$

The basic feature of the transformation of LAB to CM coordinate system is the conservation of the norm of the relative velocity vector

$$u_r = u_A - u_B = ((m_B/M)\, v_r + (m_A/M)\, v_r = v_r. \tag{10}$$

The relative translational energy of the reactants T (collision energy, CM collision energy) is then identical with the kinetic energy of the reactants in the CM system:

$$T = (1/2)\, \mu\, v_r^2 = (1/2)\, \mu\, u_r^2 \tag{11}$$

(μ is the reduced mass $\mu = m_A m_B/M$).

From the relations for u_A, u_B follows a simple form of the momentum conservation law in the CM coordinate system, namely

$$-m_A u_A = m_B u_B \tag{12}$$

Analogous relations can be derived for the products C and D [44].

The LAB scattering angle of the product C, Θ_C, can be then defined as the angle between the radius vector $\mathbf{v_C}$ and the radius vector of the reactant $\mathbf{v_A}$. It is identical with the polar angle Θ_C of the product velocity in the LAB system. Similarly, we can define the scattering angle of the product C in the CM system, ϑ_C, as the angle between the radius vectors $\mathbf{u_A}$ and $\mathbf{u_C}$; it is identical with the polar angle ϑ_C of the product velocity in the CM system.

4.3. Transformation of intensities: the probability density formalism

In addition to transformation of velocities and angles between LAB and CM systems of coordinates,

relations for transforming measured intensities must be available. One now returns to the three-dimensional systems assuming, however, that in the experiment the detection orifice is an aperture or a short slit (comparable resolution in the plane of the beams and perpendicularly to it).

In the polar LAB system the size of the volume element of the velocity space is $dv\ d\Omega = dv\ d\Theta\ d\Phi$. Similarly, the size of the volume element in the polar CM system is $du\ d\omega = du\ d\vartheta\ d\varphi$ ($d\Omega$ and $d\omega$ are elements of the LAB and CM solid angles, respectively). Thus the size of the volume elements in the LAB system increases with v^2 with the distance from the origin O and vanishes at O. Similarly, in the CM system, the size of the volume elements increases with u^2 with the distance from the origin O' and vanishes at O' (see Fig. 8). This causes difficulties in interpreting the data. Therefore, it was suggested in the early years of the scattering studies [45] to use Cartesian coordinates and a quantity called Cartesian probability to interpret the scattering data and construct the scattering diagrams. The Cartesian probability elements $dv_1\ dv_2\ dv_3 = du_1\ du_2\ du_3$ have the same size over the entire velocity space.

In the following, the probability density formalism [44] will be introduced as a consistent treatment of the measured quantities and their processing to yield further quantities characterizing the dynamics.

The following discussion refers to product ion C, unless stated differently. For simplicity, the index C will be omitted in the equations.

First, the quantity $f(v,\Omega)dvd\Omega$ will be introduced. Its meaning is the probability density distribution of the product C having in the LAB coordinates velocity in the interval (v; $v+dv$) and appearing in the LAB solid angle interval (Ω; $\Omega+d\Omega$). The variables v, Ω can be transformed to the complete set of spherical variables v, Θ, Φ. It follows from the probability conservation that

$$f(v,\Omega)\ dv\ d\Omega = f(v,\Theta,\Phi)\ dv\ d\Theta\ d\Phi, \tag{13}$$

with $f(v,\Omega)\ sin\Theta = f(v,\Theta,\Phi)$. Using the usual Jacobian transformation relations, one obtains

$$f(v,\Theta,\Phi) = v^2\ sin\Theta\ f(v_1,v_2,v_3), \tag{14}$$

where v_1, v_2, v_3 is a complete set of Cartesian coordinates of the product velocity in the LAB system. The meaning of $f(v_1,v_2,v_3)$ is the probability of the ion velocity Cartesian components falling within (v_1; v_1+dv_1), (v_2; v_2+dv_2),(v_3; v_3+dv_3).

The transformation of the LAB Cartesian coordinates v_1, v_2, v_3 into CM Cartesian coordinates u_1, u_2, u_3 gives $f(v_1,v_2,v_3) = f(u_1,u_2,u_3)$ and the transformation of the CM Cartesian coordinates u_1, u_2, u_3 to the CM spherical coordinates u, ϑ, φ leads to

$$f(u_1,u_2,u_3) = (u^2\ sin\vartheta)^{-1}\ f(u,\vartheta,\varphi) \tag{15}$$

Due to the scattering experiments usually in the LAB kinetic energy distribution of product ions, i.e. a quantity proportional to the probability density f (E , Ω),being measured, one should remember that

$$f(v,\Omega)dv\ d\Omega = f(E,\Omega)\ dE\ d\Omega \tag{16}$$

and

$$f(v,\Omega) = f(E,\Omega)\ mv \tag{17}$$

Combining the equations above, we arrive at an important relation

$$f(v,\Omega)v^{-2} = f(E,\Omega)mv^{-1} = f(v_1,v_2,v_3) = f(u_1,u_2,u_3) = (u^2\ sin\vartheta)^{-1}\ f(u,\vartheta,\varphi) \tag{18}$$

Thus by dividing the (measured) probability density $f(E,\Omega)$ by the appropriate value of the norm $v = (2E/m)^{1/2}$ one obtains a quantity proportional to the probability density $f(u_1,u_2,u_3)$. The probability density distribution $f(u_1, u_2, u_3)$ must reflect the cylindrical symmetry of the scattering pattern about the reactant relative velocity vector. This makes it possible to represent the distribution of product velocities by a cut through the velocity space of the system containing the reactant relative velocity vector, e.g., in the plane of the beams. A contour plot of the probability density distribution $f(u_1, u_2, u_3)$ is referred to as a contour scattering diagram (sometimes called also relative double-differential cross section, i.e. relative

cross section differentiated with respect to both angle and velocity). The probability density $f(u_1, u_2, u_3)$ has been referred to also as Cartesian probability [42], Cartesian intensity, flux density.

4.4. Derived dynamical quantities: probability density distribution of the CM scattering angle and of the product relative translational energy

The probability density of the CM scattering angle ϑ (refers again to the product ion C) is defined by

$$P(\vartheta) = \int u^2 f(u_1,u_2,u_3)du \tag{19}$$

It can be derived from the equations above [44] that this quantity is proportional to the differential cross section $\sigma_{diff}(\vartheta)$ and the proportionality constant is the total cross section of the process. The dependence of $P(\vartheta)$ on ϑ is sometimes referred to as CM angular distribution or relative differential cross section.

To obtain the probability density $P(T')$ of relative translational energy of the products T', we derive first the expression for the probability density $P(u)$ of the product C CM velocity u,

$$P(u) = \int\int f(u,\vartheta,\varphi)d\vartheta d\varphi = 2\pi \int f(u,\vartheta,\varphi)\, d\vartheta \tag{20}$$

Substituting from Eq. (15) the relation between $f(u, \vartheta,\varphi)$ and $f(u_1, u_2, u_3)$ gives

$$P(u) = 2\pi u^2 \int f(u_1,u_2,u_3)\, sin\vartheta d\vartheta \tag{21}$$

Because $P(u)\, du = P(T')\, dT'$, one obtains for the products C,D (of masses m_C, m_D)

$P(u_C) = P(T')\, u_C\, m_C\, M\, m_D^{-1}$ and finally

$$P(T') = 2\pi m_D (m_C M)^{-1}\, u_C \int f(u_1,u_2,u_3)\, sin\vartheta d\vartheta \tag{22}$$

The relative translational energy of the products, T', is related to u_C by $T' = m_C M(2m_D)^{-1}u_C^2$. The dependence of the probability density distribution $P(T')$ on T' is usually called the distribution of product relative translational energy.

5. Examples of beam scattering studies of ion-molecule reaction dynamics

In this section, sample results of studies of the dynamics of ion-molecule reactions will be presented to illustrate some of the achievements of the scattering studies. The emphasis of this contribution is on instrumentation and therefore no attempt will be made to discuss the conclusions on the dynamics in detail. Also, this paper concerns instrumentation used in studies of reaction dynamics and thus the examples illustrate mainly phenomena observed in scattering studies of chemical reactions of ions, i.e. bond-rearrangement processes of the type

$$A^+ + BC \rightarrow AB^+ + C \tag{23}$$

where A, B, and C are atoms of groups of atoms. Other ion-molecule collision processes will be mentioned only marginally or not at all (e.g. a large field of elastic and inelastic collisions of ions).

Of the rich variety of various chemical processes studied in crossed beam experiments, examples pertaining only to one class of elementary ion-molecule chemical reactions, namely reactions of the hydrogen-moiety transfer (H^+ or H-atom), were selected. Basic phenomena observed in studies of reaction dynamics can be conveniently illustrated on this particular class of chemical reactions of ions.

5.1. Direct processes

Fig. 9 shows the scattering diagram of HeH^+ [46] formed in the reaction of H_2^+ with He at the collision energy of 2.70 eV (cm), with the underlying framework of the Newton diagram. The cross denotes the position of the center-of-mass (the tip of the CM vector V). In the CM coordinates, the neutral reactant He approaches from the right along the relative velocity v_r with its CM velocity u(He) (smaller of the two). The product HeH^+ is scattered preferentially forward with respect to the direction of approach of the reactant He, the backward scattering representing only 14% of the forward peak. The crater in the scattering diagram about the CM point indicates

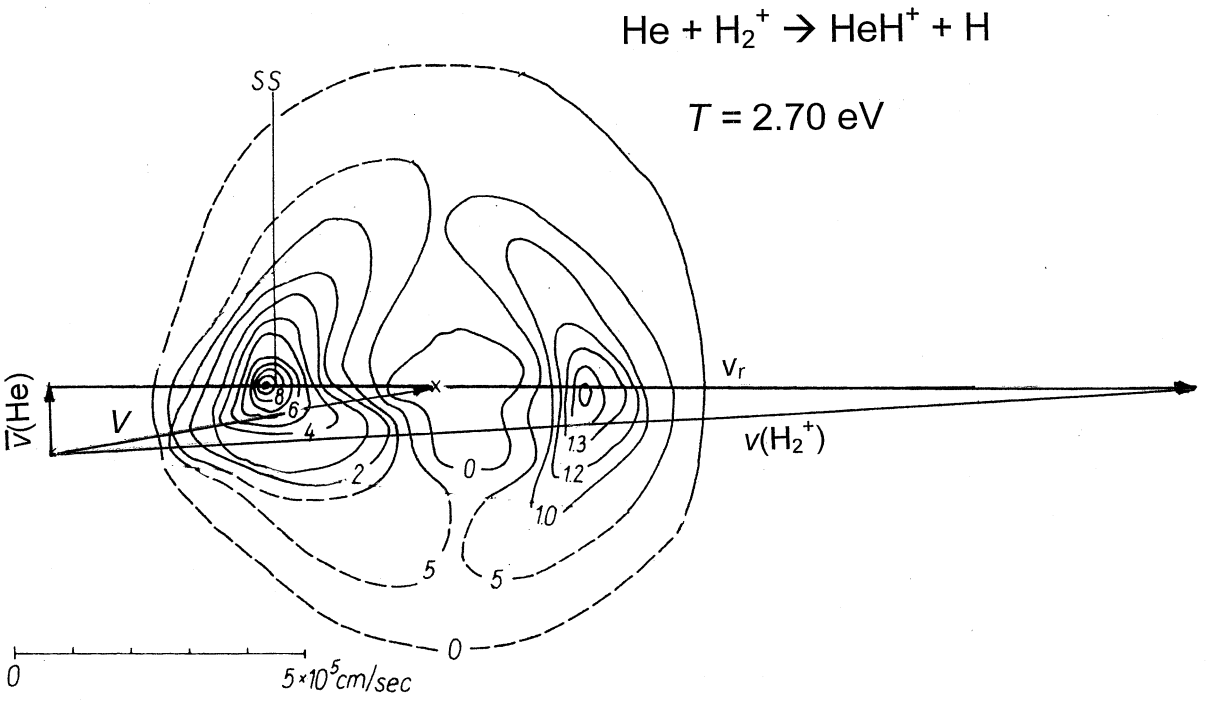

Fig. 9. Direct mechanism: Newton diagram for the reaction H_2^+ + He at T =2.70 eV and the contour scattering diagram of the product HeH^+ (adapted from author's data in [44]). For more details see the text.

dissociation of the reaction product excited above the dissociation limit (low CM velocity means high internal excitation). The preferential scattering of HeH^+ in one direction with respect to the CM point (a strong forward-backward asymmetry) characterizes a direct (impulsive) collisional mechanism of proton transfer in which the reactants interact for a period of time shorter that a vibrational period of the system. Peaking of the product close to the point spectator stripping (SS) suggests that the direct mechanism can be described by the SS model in which the peak product velocity is determined by a simple momentum transfer of the proton of H_2^+ to the momentum of the projectile He moving in the opposite direction. This conclusion was confirmed by an accompanying quasiclassical trajectory study [46] on the ground-state HeH_2^+ potential energy hypersurface, one of the first trajectory studies of ion-molecule reactions. The calculations showed that typical reactive trajectories are of a direct, unsnarled type, close to the spectator stripping model predictions. The dynamical quantities, which could be derived from both experiment and theory (product CM angular distributions and relative translational energy distributions), were in excellent agreement.

Another example of the direct, stripping mechanism is the reaction between Ar^+ and hydrogen (deuterium). In Fig. 10, the scattering diagram of ArD^+ formed in this reaction at the collision energy of 2.72 eV (cm) is shown [47]. The direction of the relative velocity is along the axis 180°–0° and the projectile Ar^+ approaches from the left. The product is preferentially scattered forward with respect to the CM point (cross in Fig. 10), indicating a direct process. This reaction was studied by many laboratories and other measurements [48] confirmed that the forward scattering of the product and the direct character of the process persists even at collision energies approaching the thermal region (0.08 eV, CM). It turns out that the direct character of a process is connected with the type of the potential energy hypersurface of the system: direct processes are con-

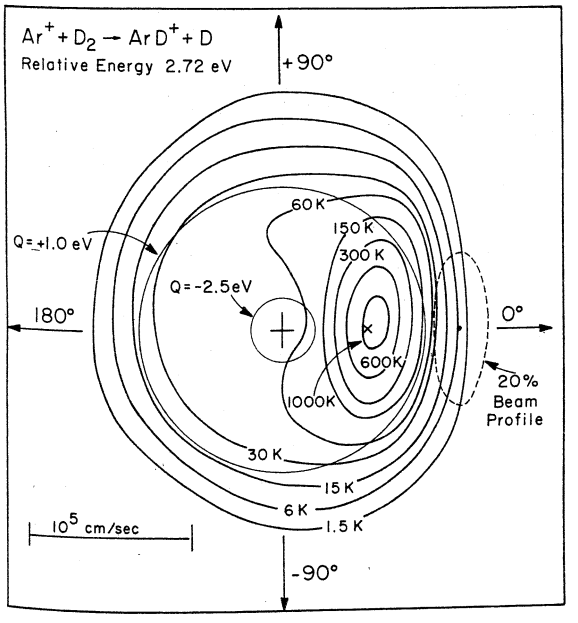

Fig. 10. Direct mechanism: Contour scattering of ArD^+ formed in the reaction between Ar^+ and D_2 at $T = 2.72$ eV [45].

nected with hypersurfaces relatively flat in the interaction region along the direction of the reaction coordinate.

5.2. Intermediate complex formation and decomposition

An indication that in a chemical reaction a long-lived intermediate complex is formed from the reactants, which then decomposes to products, is the symmetry of the scattering diagram of the product with respect to a plane passing through the center-of-mass point perpendicularly to the relative velocity. Such a behavior results from the formation of an intermediate species (thermodynamically stable with respect to both reactants and products), which lives for many rotations, and then it decomposes in a unimolecular way randomly, without preference to any direction. The important difference between a unimolecular decomposition of an excited molecule and unimolecular decomposition of this reaction intermediate is a high angular momentum of the latter; this comes mainly from the orbital angular momentum of the approaching reactants. Deposition of the angular momentum determines the detailed shape of the CM angular distribution which is, however, always symmetric with respect to the CM scattering angle of 90° (reflection of the specific shape of the scattering pattern). In an ideal case, a statistical complex is formed which redistributes randomly the energy available over its internal degrees of freedom and then it decomposes with an exponential distribution of lifetimes to products. Thus the characteristics features of the intermediate complex formation and decomposition in scattering are (a) forward-backward symmetry of the scattering pattern, and (b) deposition of only a small fraction (on the average) of the energy available in the process into the product relative translational energy. The shape of the product relative translational energy distribution curve results from the statistical distribution of energy over the internal degrees of freedom of the intermediate under the condition of the total angular momentum conservation. Complex-forming collisions are thus strongly inelastic. The forward-backward symmetry of the scattering pattern has a tendency to decrease, if the mean lifetime of the intermediate approaches one or a few mean rotations. This may be sometimes used to roughly estimate the mean lifetime of the intermediate.

Fig. 11 shows, as an example, scattering patterns of C_3HD^+ and $C_3D_2^+$ (relative concentrations of the two products indicated statistical H-D scrambling) from the reaction of C_3H^+ and D_2 [49]. The scattering pattern exhibits, within the experimental error, the forward-backward symmetry and it is somewhat elongated along the axis perpendicular to the relative velocity (horizontal line). This suggests a dissociating intermediate which behaves as a oblate near-symmetric top, and leads to the conclusion that the critical configuration of the intermediate, from which the products are formed by an extension of a critical bond, is prevailingly a cyclic $C_3HD_2^+$ structure decomposing to a cyclic product c-C_3HD^+ (c-$C_3D_2^+$) and a D(H) atom [49].

One of the decomposition paths of an intermediate complex must be its dissociation backward to the

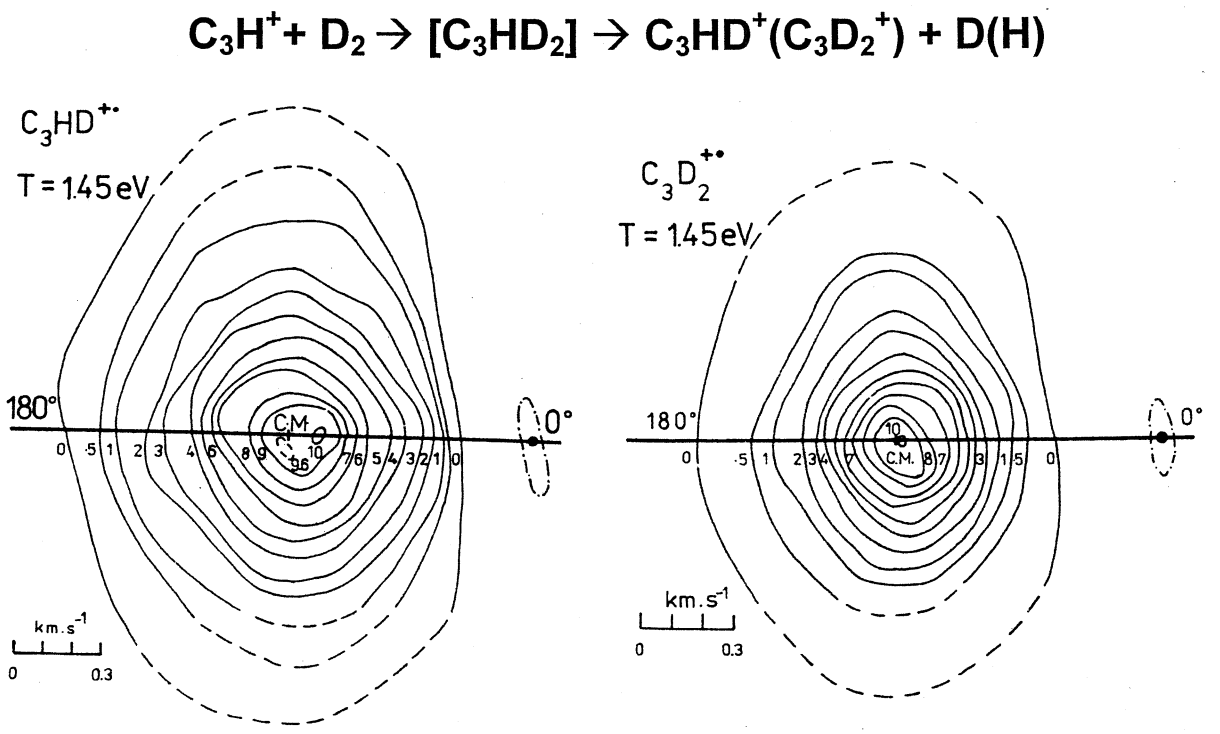

Fig. 11. Intermediate complex formation: Contour scattering diagrams of C_3HD^+ and $C_3D_2^+$ from the reaction $C_3H^+ + D_2$ at $T = 1.45$ eV (adapted from data in [47]).

reactants. Fig. 12 brings an example of scattering results on such a decomposition channel: the reaction between the acetylene cation and acetylene molecule leads to reaction product ions $C_4H_3^+ + H$, and $C_4H_2^+ + H_2$. Using $C_2D_2^+ + C_2H_2$ as reactants reveals formation of C_2HD^+, formed as a result of H-D scrambling in an intermediate $C_4H_2D_2^+$ and its decomposition backwards to the reactants [50]. The scattering pattern has the forward-backward symmetry indicative of an intermediate complex formation, but it is extremely elongated along the relative velocity - an entirely different shape from that in Fig. 11. This shape is consistent with the intermediate having a practically linear C-C-C-C shape in the critical configuration leading backward to the reactants. The translational energy distribution peaks at 0.15 eV, i.e. at about 6% of the total energy available in this reaction channel showing a strongly inelastic process of a statistical complex decomposition.

5.3. Parallel mechanisms

Some ion-molecule reactions were shown to proceed by several parallel collision mechanisms. The reaction between the methane cation and methane molecule leading to CH_5^+ belongs to the oldest and most often studied ion-molecule reactions. Scattering studies of its dynamics revealed, however, that its collisional mechanism is rather complicated. Fig. 13 shows a scattering diagram of CH_5^+ at the collision energy of 0.67 eV [51]. It shows three groups of the product ions CH_5^+ which can be identified with three parallel mechanisms of the product formation: (a) direct mechanism of proton transfer from CH_4^+ to CH_4 with characteristics of the spectator stripping mechanism (P_{SS} in the lower portion of Fig. 13); (b) direct mechanism of H-atom transfer from CH_4 to CH_4^+, again with an energy release characteristic of the stripping mechanism (H_{SS} in the figure); (c) an

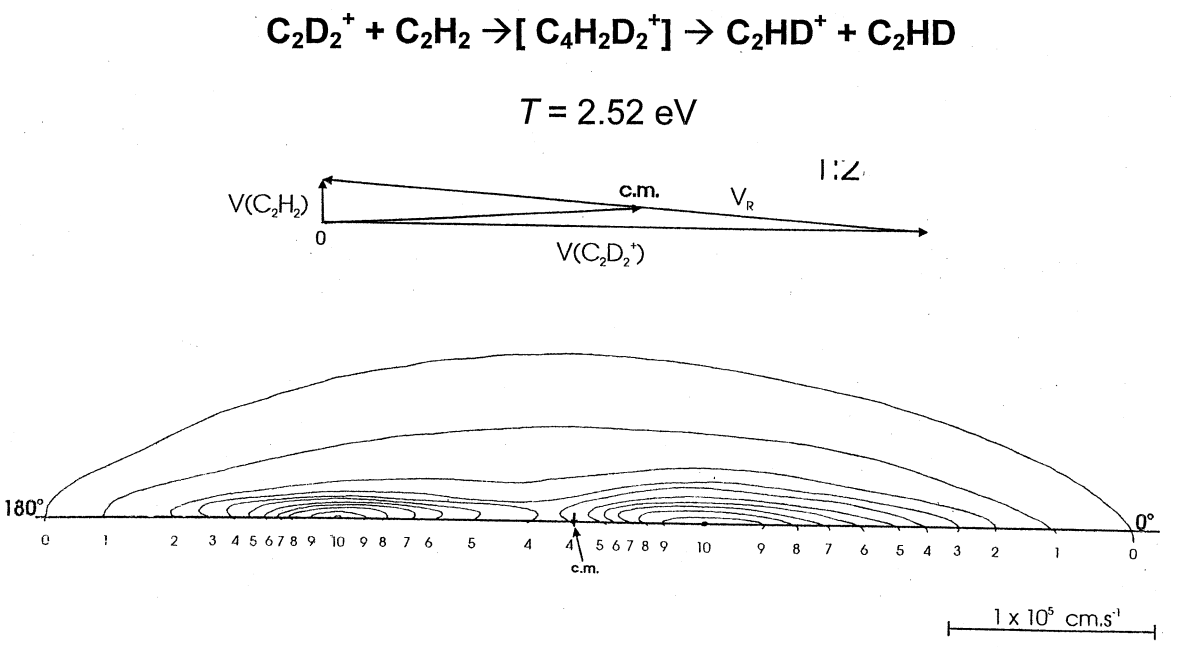

Fig. 12. Intermediate complex formation: Contour scattering diagram of C_2HD^+ from backward decomposition of the intermediate complex formed in $C_2H_2^+ + C_2H_2$ collisions at $T = 2.52$ eV (adapted from data in [48]).

intermediate long-lived complex $C_2H_8^+$ decomposition (intensity symmetrically distributed about the CM point, indicating a strongly inelastic reactive process,. typical for dissociation of an intermediate). Formation of products by these three parallel mechanisms appears to be a general phenomenon in reactions between hydrogen-containing molecular cations with their own molecules, observed since in several other systems (water, acetonitrile, methanol, acetone).

An example of different reaction paths on a potential energy hypersurface of a system, leading to the same product, may be the reaction between the acetylene cation and methane leading to $C_2H_3^+$ and CH_3 [52]. The scattering pattern of $C_2H_3^+$ (Fig. 14) exhibits two pairs of peaks symmetrically located forward and backward from the CM point along the relative velocity. The two inner peaks have the same height, while the outer pair of peaks exhibits an asymmetry: the backward peak is about half of the forward peak. This pattern and its dependence on the collision energy was interpreted as indicating formation of the product simultaneously via decomposition of intermediates of two different lifetimes, connected with two different pathways on the potential energy hypersurface. Formation of the long-lived intermediate (estimated mean lifetime longer than about 4 ps) suggests a reaction path involving formation of strongly-bound $C_3H_6^+$ isomers, and formation of the shorter-lived intermediate (mean lifetime decreasing to about 0.3 ps at the collision energy shown in Fig. 13) as a reaction path going through H-bonded intermediates $(C_2H_2..H..CH_3)^+$. This conclusion was further confirmed by results of studies of the reaction with CD_4: the lower part of Fig. 13 shows velocity profiles along the relative velocity of the ion products with increasing H-D exchange, $C_2H_2D^+$, $C_2HD_2^+$, $C_2D_3^+$, respectively. It can be seen that the inner peaks (long-lived complex) remain practically unchanged with the extent of H-D scrambling, while the outer peaks (shorter-lived intermediate) gradually disappear with increasing H-D scrambling. This indicates that the rate of the decomposition of the shorter-lived intermediate effectively competes with the rate of H-D scrambling. The lower part of Fig. 14 shows also

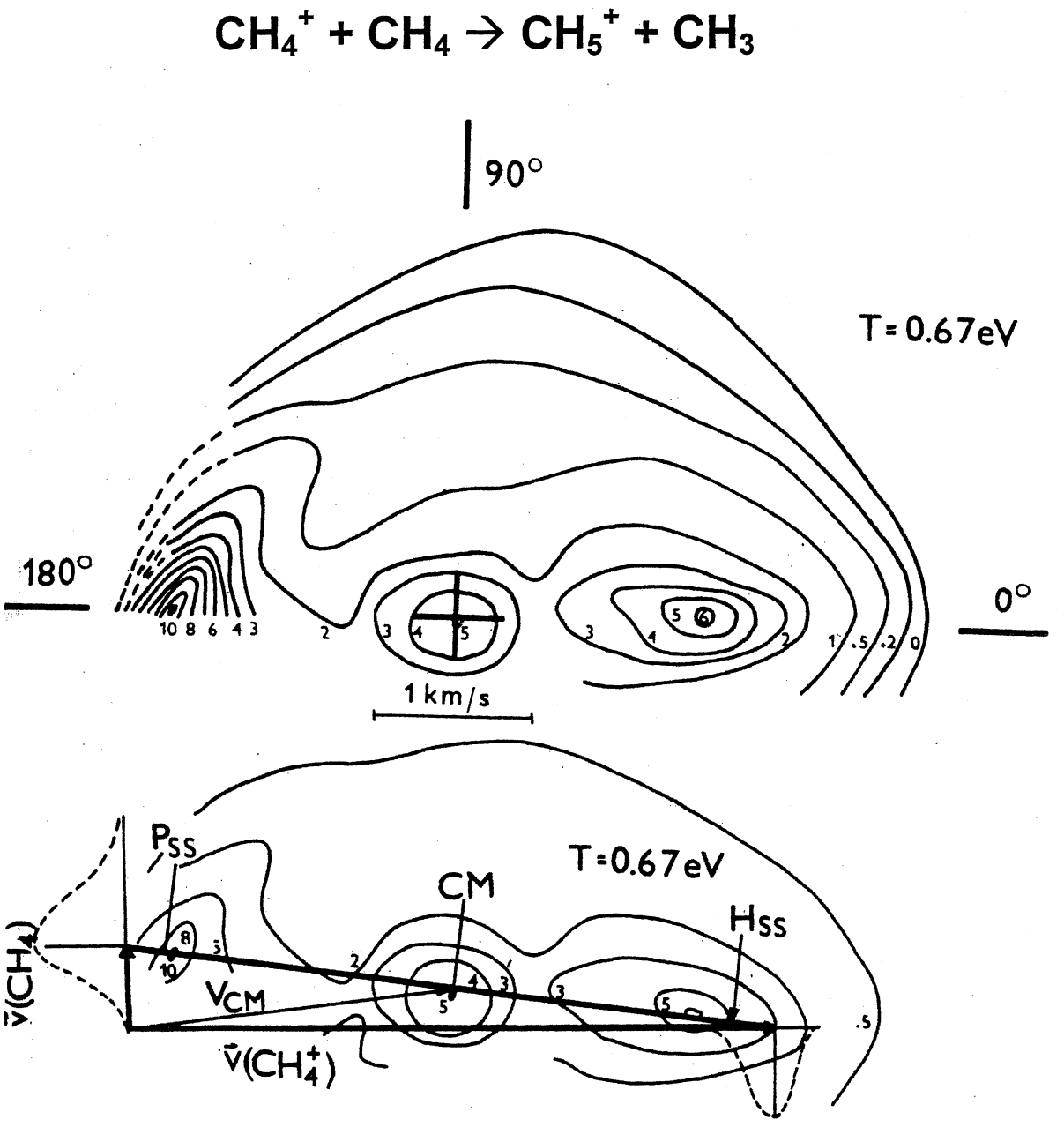

Fig. 13. Parallel mechanisms: Contour scattering diagram of CH_5^+ formed in $CH_4^+ + CH_4$ collision at $T = 0.67$ eV (upper part), and (lower part) the respective Newton diagram with beam velocity spreads, schematics of the CH_5^+ contours and mechanism indications (P_{SS} - proton stripping, H_{SS} - H-atom stripping, CM - center-of-mass).

results of velocity distribution of the three products as obtained in a guided-beam experiment [53] at the same collision energy (dash-and-dot curves). The comparison of both results show that the beam scattering experiments, which relate to a thin slice of the velocity space in the plane of the beams, may sometimes provide a more detailed picture than guided beam experiments (without angular information),

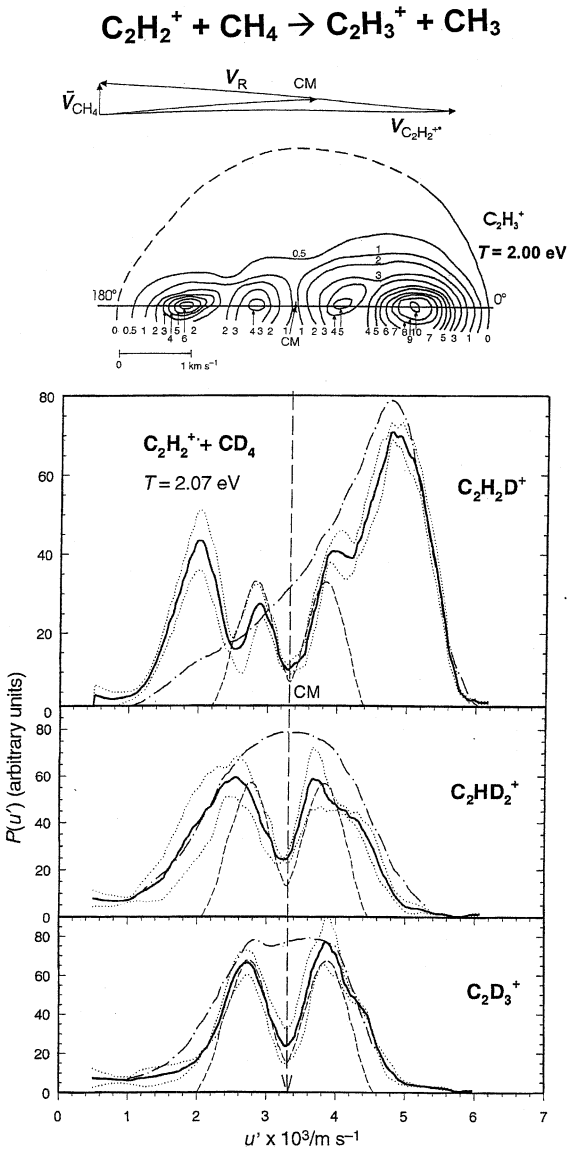

Fig. 14. Newton diagram and contour scattering diagram of $C_2H_3^+$ from reaction $C_2H_2^+ + CH_4$ at $T = 2.00$ eV (upper part). Velocity profiles along the relative velocity of reaction products $C_2H_2D^+$, $C_2HD_2^+$, and $C_2D_3^+$ from the analogous reaction with CD_4 (dash-and-dot lines show results of product velocity measurements from a guided-beam experiment at the same collision energy) - lower part (adapted from data in [50]).

which integrate over the azimuthal angle all product intensities having the same velocity component along the relative velocity vector.

5.4 High-resolution studies

Several studies of the dynamics of ion-molecule chemical reactions, in which population of internal (vibrational and rotational) states of the product was resolved in product translational energy measurement, exemplify the extent of detailed information that may be obtained from crossed-beam scattering experiments. Rather naturally, these beautiful results have been so far limited to special cases of triatomic systems. In many other cases, especially in polyatomic systems, the internal level mixing in chemical-rearrangement processes leads to population of many overlapping rotational and vibrational levels and thus attempts to resolve structure in translational energy distributions are in principle difficult.

The benchmark example of a high-resolution scattering study is the investigation of the exchange reaction $H^+ + D_2 \rightarrow D^+ + HD$ ([12,32], see also Sec. 3.3.) at low collision energies. Fig. 15 shows energy profiles of the product D^+ with partly resolved structure of the rotational and vibrational states of the neutral product HD (as indicated by arrows). At T= 0.56 and 0.64 eV shown in the figure, the collision energy is varied near the threshold of producing HD ($v = 1$). Upper part of Fig. 15 brings experimental results, its lower part compares the results with rovibrational distributions as calculated using the most dynamically biased (MDB) variation of the statistical model [54]. The overall agreement between the experiment and calculations (assuming a statistical intermediate) on the population of product internal states indicates involvement a strongly bound intermediate HD_2^+ in the reaction.

Another remarkable series of recent high-resolution studies represents investigation of reactions of simple anions at low collision energies. Fig. 16 summarizes the results of studies of the reaction between O^- and D_2 [55]. Structure observed in the translational energy distributions of the product OD^- was deconvoluted and plotted as a fine-structured scattering diagram. From it, relative populations of the vibrational levels of OD^- and vibrational-state dependent angular distributions could be derived as well as their changes with the collision energy. Such

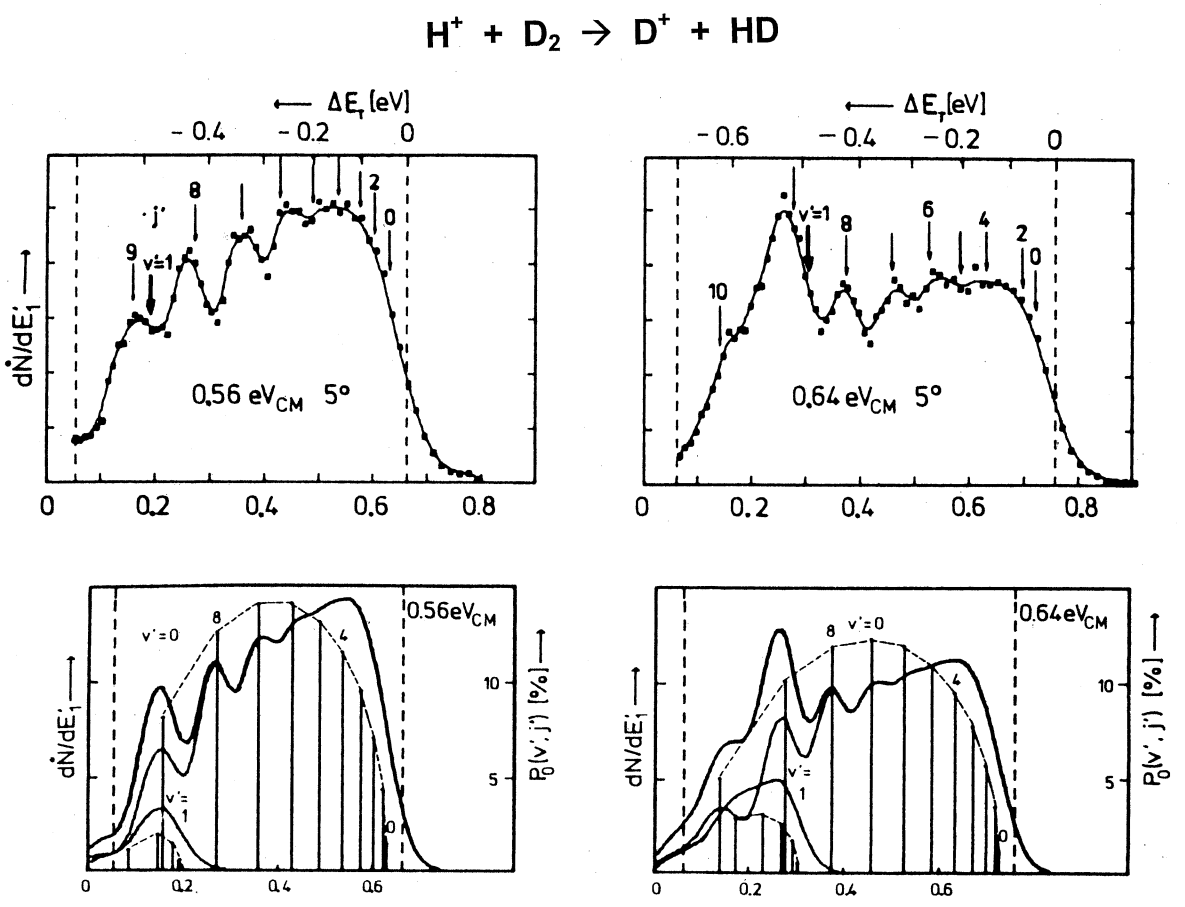

Fig. 15. Energy profiles of D^+ (at the LAB scattering angle of 5°) from the hydrogen exchange reaction in $H^+ + D_2$ collisions at low energies (0.56 and 0.64 eV) with arrows pointing to positions of vibrational (v′) and rotational (j′) levels of HD formed (upper part). Lower part: fit of the experimental data using the statistical MDB model (sticks and dashed line). Adapted from [32], see also [12].

fine experimental information provides an excellent basis for very detailed dynamical conclusions and a challenge for further theoretical studies.

5.5. Chemical reactions of molecular dications

While elementary processes of charge transfer between doubly charged ions and neutral molecules have been investigated for several decades and their dynamics and energy partitioning in products studied in detail in scattering experiments [56,57], observation of chemical reactions of molecular dications is a fairly recent phenomenon [58]. Beam scattering studies of the reaction between $CF_2^{2+} + D_2$ [59,60] provide information on the dynamics of the main processes, a chemical reaction leading to $CF_2D^+ + D^+$ (exoergicity $-\Delta H_R = 7.6$ eV) and a nondissociative charge-transfer reaction leading to $CF_2^+ + D_2^+$ ($-\Delta H_R = 5.04$ eV). The scattering diagrams of the products CF_2D^+ and CF_2^+ (Fig. 17) show the products recoiling with substantial velocity and indicate that coulomb repulsion between two singly charged reaction products dominate the energy partitioning. The peaks in product translational energy distributions show that in the charge transfer process with highest probability 4.1–4.5 eV (about 76% of total energy available) goes into product translation, about 1 eV goes into internal excitation of the CF_2^+ product, and

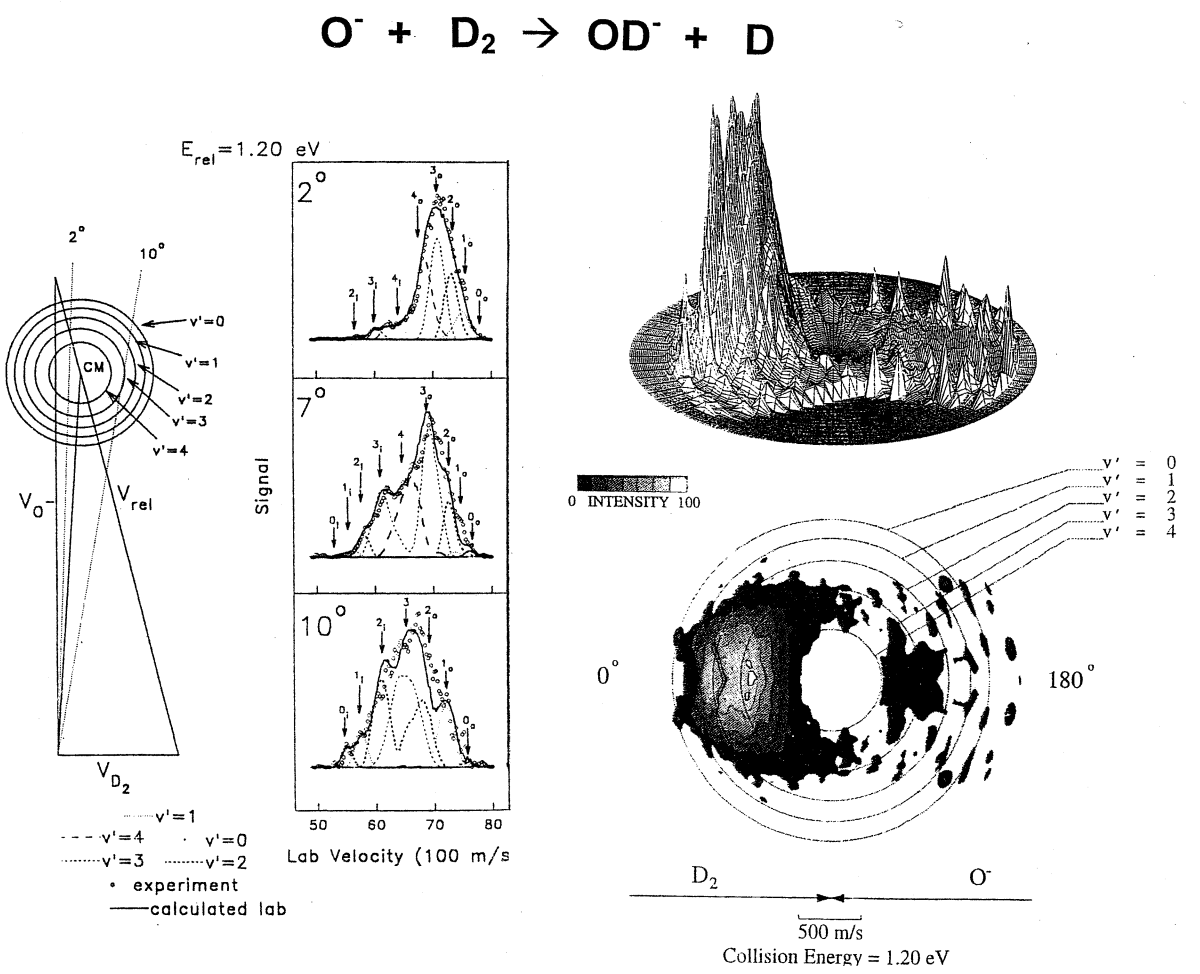

Fig. 16. Summary of scattering results on OD^- formed in $O^- + D_2$ collisions at $T = 1.20$ eV. Left: Newton diagram and LAB velocity profiles of OD^- at several scattering angles. Right: contour scattering diagram and 3D scattering diagram derived from the data (adapted from [52]).

about 0.25 eV into internal excitation of the D_2^+ product ($v = 1,2$). In the chemical reaction, 6–6.5 eV (about 75% of the total energy available) results in product translation and 1.7–2.7 eV (about 25%) remains as internal excitation of the molecular product. For a chemical reaction, this is an unusually high fraction of energy in translation and thus the chemical reactions of dications appear to represent a new, rather unusual class of chemical reactions, characterized by a very high kinetic energy release. Also, this and other reactions of molecular dications with hydrogen belong to a very rare type of chemical reactions of ions in which a "naked" proton (and, in addition, of a high kinetic energy) is formed. A general model, based on crossings of potential energy surface(s) of the dication system with coulomb repulsive surfaces leading either to charge transfer or to chemical rearrangement products was suggested [59,60] which accounts well for the competition of various processes observed in dication-neutral collisions.

5.6. Dynamics of charge transfer processes

Scattering studies contributed also to better understanding of the dynamics and energy exchange in

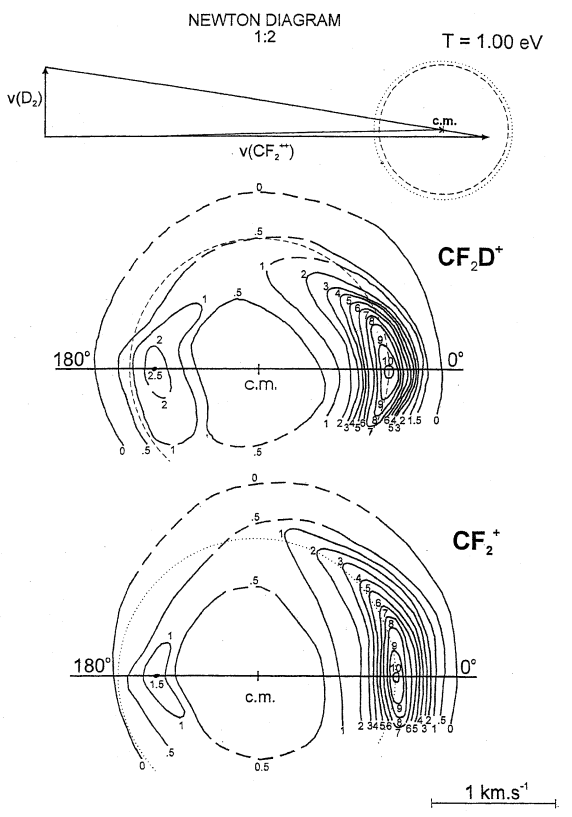

Fig. 17. Chemical reactions of molecular dications: Scattering diagrams of the products CF_2D^+ and CF_2^+ from CF_2^{2+} + D_2 collisions at T = 1.0 eV. The upper part of the figure gives the underlying Newton diagram (in the reduced scale 1:2); circles show the maximum CM velocity the products CF_2D^+ (dashed) and CF_2^+ (dotted) can achieve, if the exoergicity of the process were transformed entirely into product translational energy (adapted from [60]).

cation-neutral charge transfer processes. Some of the results will be mentioned at least briefly here. Early studies showed that the translational-to-internal energy exchange in elementary charge transfer processes varies considerably with the impact parameter of the reactants: for large impact-parameter collisions, which lead to little or no angular deflection of the charge-transfer products, the process tends to occur by a simple electron jump in a near-resonant way. On the other hand, small impact-parameter collisions lead to large-angle scattering and to a considerable momentum exchange which may populate many internal states of the products (if an intermediate is formed in this latter collision, a considerable level mixing and population of a wide range of internal states may occur). Fig. 18 shows, as an example, scattering results on a charge transfer study of a simple system $Ar^+(H_2, Ar)\ H_2^+$ system, i.e. collisions of $Ar^+ + H_2$ leading to $H_2^+ + Ar$ (see Sec. 5.1. for dynamics of a chemical reaction in this system). Fig. 18 (upper part) shows a scattering diagram of H_2^+ at the collision energy of 0.48 eV: 0° indicates the direction of the ion product H_2^+ which did not suffer any deflection in the charge transfer process (original direction of movement of the neutral reactant). Maximum of the scattered intensity occurs about this point, practically on the resonant charge transfer (RCT) circle, which indicates the loci of the product velocity, if no exchange between translational and internal degrees of freedom of the system took place. The much smaller backward scattering shows a broader distribution of product velocities and its maximum occurs inside the RCT circle, indicating a translationally endoergic process. The lower part of Fig. 18 gives the product relative translational energy distribution, resulting from small angle scattering (over $0° \leq \vartheta \leq 60°$), for three collision energies between 0.13 and 3.44 eV. The scales in the upper part of the figure indicate the translational energy release expected for the formation of H_2^+(v, J). The result clearly shows that over a wide collision energy range for small angle scattering (large impact parameters and small angular deflections) the charge transfer process occurs preferentially without momentum exchange in a resonant way, leading with $Ar^+(^2P_{3/2})$ to the formation of $H_2^+(v = 1)$ with no or very little change of the rotational state of the molecular species. For large angle scattering (Fig. 18, lower part, right) a broad range of vibrational and rotational states is populated in momentum exchange, inelastic and superelastic charge transfer collisions, resulting from small impact-parameter, intimate (though still prevailingly direct) encounters. The discussed case represents a very simple system with rather widely separated internal states. For a polyatomic system with a high density of internal states of the molecular product, a rather narrow band (a few tens of an eV) of internal states about the resonant energy tends to be populated

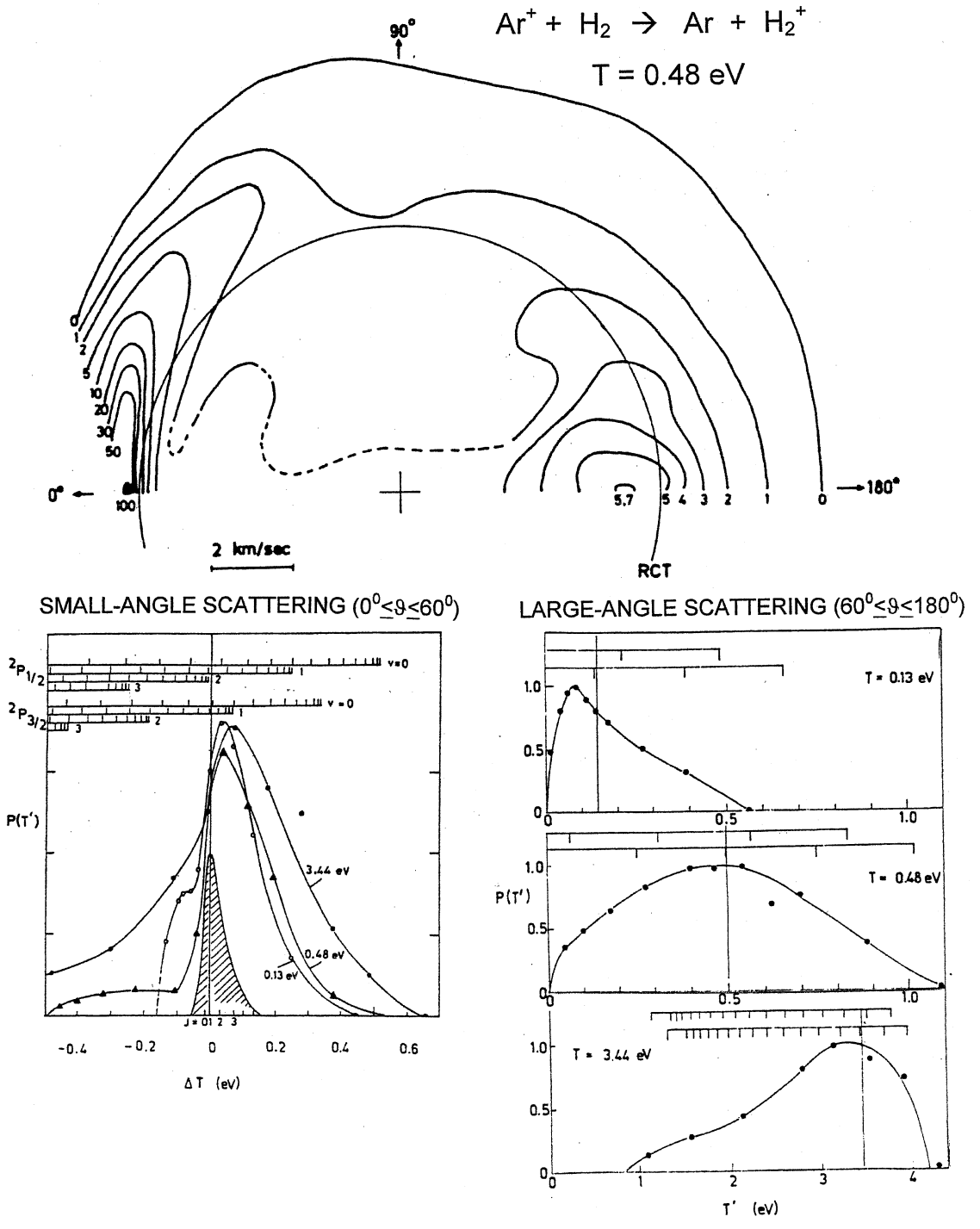

Fig. 18. Charge transfer $Ar^+(H_2, Ar)H_2^+$: the upper part shows the scattering diagram of H_2^+ at $T = 0.48$ eV, the lower part product translational energy distribution for three collision energies between 0.3 and 3.44 eV for small angle scattering (left, plotted against translational exoergicity $\Delta T = T'\text{-}T$), and large-angle scattering (right, plotted against T'. The scales show product translational energy expected for H_2^+ formed in the respective vibrational (rotational) states (adapted from data in [61]).

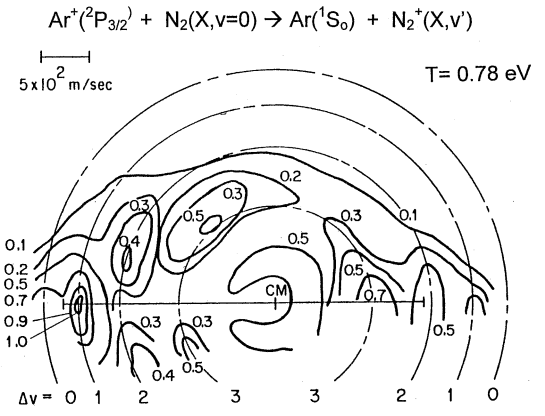

Fig. 19. Charge transfer $Ar^+(N_2, Ar)N_2^+$: scattering diagram of N_2^+ at $T = 0.78$ eV; concentric circles about CM indicate velocities of the ion product, if formed in the respective vibrational states $N_2^+(v')$. Adapted from [64].

in large impact parameter, simple electron exchange collisions, as shown, e.g. in a scattering study of the charge transfer between Kr^+ and CH_4 [62].

Considerable amount of attention was given to the charge transfer process $Ar^+(N_2, Ar)N_2^+$, in particular to the probability of formation of specific vibrational states of N_2^+. Various experimental and theoretical methods were used to address this problem [63]. In beam scattering studies of this reaction [64], structures in the scattering diagrams were resolved which could be correlated with the formation of N_2^+ in various vibrationally excited states. Fig. 19 is an example of a scattering diagram at the collision energy of 0.8 eV. Concentric circles about the CM point correspond to loci of formation of the ion product $N_2^+(X^2\Sigma_g)$ in v = 1, 2, 3 in processes of endoergicities increasing from 0.09 eV (v = 1); Formation of N_2^+(v = 0) in a slightly exoergic process (by 0.18 eV) was also observed. Relative populations of the ion product vibrational states could be derived from the scattering diagrams as well as their changes with the collisions energy. The scattering data contributed significantly to understanding of the state-to-state dynamics of this system.

High-resolution scattering experiments on the charge transfer process $H^+ + O_2$ [29,65] revealed a strong dependence of the vibrational transition probabilities to O_2^+(v) on the scattering angle. At very low laboratory scattering angles a strongly enhanced contribution of the more resonant states (v = 3–6) was found (as compared to a Franck–Condon distribution). The Franck–Condon distribution peaks at v=1 and population of vibrational states about this value was reflected in the measured spectra at scattering angles of about 4°, while at larger scattering angles deviations toward population of higher vibrationally excited states were observed. Explanation of the changes in vibrational state populations was given in terms of the underlying potential energy surfaces.

5.7. Dissociative scattering

Investigation of dissociative scattering, or collision-induced-dissociation (CID) with product ion energy and angle measurements, belongs to the general area of studies of inelastic (translational-to-internal) energy transfer in ion-molecule collision. The full kinematics of collision-induced dissociation processes of the type $AB^+ + C \rightarrow A^+ + B + C$, from which three products result, cannot be decided by measuring data of only one (ion) product, unless a certain assumption about the mechanism of the process is made. This may be done, e.g. for polyatomic projectiles, if one can assume (on the basis of experimental evidence) that the dissociation process occurs in a unimolecular way after the energy transfer interaction with C and/or if the mass ratio A^+/B is conveniently high so that the position of A^+ in the velocity space traces at least approximately the position of collisionally-excited AB^+ before dissociation.

Collision-induced-dissociation at keV energies, besides being a significant source of information on energetics and collision mechanism of small molecular projectiles [66], has been for a long time an extremely important mass spectrometric tool in structural and analytical characterization of large polyatomic ions [67]. An important observation of the dependence of the extent of parent ion fragmentation on the scattering angle for keV projectiles [68,69] brought up the question of the energy-transfer vs. angle correlation. An early crossed-beam scattering study of this problem [70] established even for low

CM collision energies (a few eV) of simple polyatomic projectile ions (CH_4^+, $C_3H_8^+$) a unimolecular character of the decomposition of the collisionally activated projectile, an approximately linear dependence between the most probable energy transferred and the CM scattering angle, and the translational-to-vibrational character of the energy transfer. Also, the basic kinematic charactertistics of the dissociative scattering were formulated. Further low-energy dissociative scattering studies have provided data on long-lived isolated electronic states of polyatomic projectiles [71,72] and a knockout mechanism in dissociation of small molecular ions [73]. A recent review [74] summarizes the results of low-energy dissociative scattering studies in context with other methods of investigation of dissociation of ions by collisional activation. The guided-beam technique with angular analysis has been recently applied to studies of CID to determine the $(CO)_5Cr^+$–CO bond dissociation energy [75].

6. Conclusions

This is a shortened review on the instrumentation used in beam scattering experiments in ion-molecule reaction dynamics, complemented by selected examples of some of the processes studied and dynamical conclusions achieved. Investigation of the dynamics of ion-molecule processes, i.e. of collision mechanisms and energy partitioning in products, has represented and will undoubtedly represent just a small part of studies of ion-molecule reactions. One of the reasons is that experiments are difficult and time consuming. A more important reason appears to be that there will be always much larger demand for kinetic data on ion-molecule processes: values of rate constants and their temperature dependence, cross sections and their dependence on energy, possibly influence of selective energy of the reactants on rate constants and cross sections. Nonetheless, when it comes to detailed understanding of an elementary process, i.e. the influence of selected energy of reactants on collisional mechanism and on energy partitioning in the products, crossed beam scattering experiments are most likely to provide the answer.

Acknowledgements

This paper is dedicated to Graham R. Cooks on the occasion of his sixtieth birthday as an expression of respect to his personality and to his manifold contributions to ion chemistry and mass spectrometry. The author gratefully acknowledges the award of a JILA Visiting Fellowship of (January–July, 2001) during which most of the manuscript was prepared. The work was partially supported by Grant No. 203/00/0632 of the Grant Agency of the Czech Republic.

References

[1] V.L. Talrose, A.A. Lyubimova, Dokl. Acad. Nauk SSSR 86 (1952) 909.
[2] F.H. Field, J.L. Franklin, F.W. Lampe, J. Am. Chem. Soc. 78 (1956) 5697.
[3] E.E. Ferguson, in Ion/Molecule Reactions, J.L. Franklin, (Ed.), Plenum, New York, 1972, Vol. 2, p.363.
[4] D. Smith, N. Adams, in Gas Phase Ion Chemistry, M.T. Bowers, (Ed.), Academic Press, New York, 1979, Vol. 1, p.1.
[5] J.M.S. Henis, in Ion-Molecule Reactions, J.L. Franklin, (Ed.), Plenum, New York, 1972, Vol. 2, p.395.
[6] Z. Herman, R. Wolfgang, in Ion-Molecule Reactions, J.L. Franklin, (Ed.), Plenum, New York, 1972, Vol. 2, p.553.
[7] W. Koski, in Advances in Chemical Physics, K.P. Lawley (Ed.), Wiley, NewYork, 1975, Vol. XXX, p. 185.
[8] W.R. Gentry, in Gas Phase Ion Chemistry, M.T. Bowers (Ed.), Academic Press, New York, 1979, Vol. 2, p. 221.
[9] Gaseous Ion Chemistry and Mass Spectrometry, J.H. Futrell, (Ed.),Wiley, New York, 1986.
[10] Techniques for Studies of Ion-Molecule Reactions, J.M. Farrar, W.H. Saunders, Jr. (Eds.), Wiley, New York, 1988, p.325.
[11] R.H. Neynaber, Advances in Atomic and Molecular Physics, Academic Press, New York, 1969, Vol. 5, p.57.
[12] D. Gerlich, in Advances in Chemical Physics (State-Selected and State-to-State Ion-Molecule Reaction Dynamics: Experiment), C.Y. Ng, M. Baer (Eds.), Wiley, New York, 1992, Vol. LXXXII, p.1.
[13] E. Teloy, D. Gerlich, Chem. Phys. 4 (1974) 417.
[14] Ch. Ottinger, in Gas Phase Ion Chemistry, M.T. Bowers (Ed.), Academic Press, New York, 1984, Vol. 3, p.249.
[15] Z. Herman, J.D. Kerstetter, T.L. Rose, R. Wolfgang, Rev. Sci. Instrum. 40 (1969) 538.
[16] W.R. Gentry, E.A. Gislason, B.H. Mahan, Chi-Wing Tsao, J. Chem. Phys. 49 (1968) 3058.

[17] M. Menzinger, L. Wahlin, Rev. Sci. Instrum. 40 (1969) 102.
[18] Advances in Chemical Physics (State-Selected and State-to-State Ion-Molecule Reaction Dynamics: Experiment), C.Y. Ng, M. Baer (Eds.), Wiley, New York, 1992, Vol. LXXXII, p.1.
[19] R.J. Morrison, W.E. Connaway, T. Ebata, R.N. Zare, J. Chem. Phys. 84 (1986) 5527 and references therein.
[20] Z. Herman, M.J. Henchman, B. Friedrich, J. Chem. Phys. 93 (1990) 4916.
[21] R.J. Cotter, W.S. Koski, J. Chem. Phys. 59 (1973) 784.
[22] C.R. Blakely, M.L. Vestal, J.H. Futrell, J. Chem. Phys. 66 (1977) 2392.
[23] J.C. Tully, Z. Herman, R. Wolfgang, J. Chem. Phys. 54 (1971) 589.
[24] Z. Herman, V. Pacak, Int. J. Mass Spectrom. Ion Phys. 24 (1977) 355.
[25] R.L. Champion, L.D. Doverspike, T.L. Bailey, J. Chem. Phys. 45 (1966) 4377.
[26] G. Bosse, A. Ding, A. Henglein, Ber. Bunsenges. Phys. Chem. 75 (1971) 413.
[27] R.M. Bilotta, F.N. Preuninger, J.M. Farrar, J. Chem. Phys. 73 (1980) 1637.
[28] C.R. Blakely, P.W. Ryan, M.L. Vestal, J.H. Futrell, Rev. Sci. Instrum. 47 (1974) 15.
[29] J.P.Toennies, G.Niedner-Schattenburg, in Advances in Chemical Physics (State-Selected and State-to-State Ion-Molecule Reaction Dynamics: Experiment), C.Y. Ng, M. Baer (Eds.), Wiley, New York, 1992, Vol. LXXXII, p. 553.
[30] V. Hermann, H. Schmidt, F.Linder, J. Phys. B 11 (1978) 493.
[31] K.L. Wendel, C.A. Jones, J.J. Kaufmann, W.S. Koski, J. Chem. Phys. 63 (1975) 750.
[32] D. Gerlich, Thesis, University of Freiburg, 1977.
[33] Z. Herman, K. Birkinshaw, Ber. Bunsenges. Phys.Chem. 77 (1973) 566.
[34] M. Barat, J.C. Brenot, J.A. Fayeton, J.C. Houver, J.B. Ozenne, R.S. Berry, M.Durup-Ferguson, Chem. Phys. 97 (1985) 165.
[35] J.C. Brenot, M. Durup-Ferguson in Advances in Chemical Physics (State-Selected and State-to-State Ion-Molecule Reaction Dynamics: Experiment), C.Y. Ng, M. Baer (Eds.), Wiley, New York, 1992, Vol. LXXXII, p. 309.
[36] N.R. Daly, Rev. Sci. Instrum. 31 (1960) 264.
[37] B.R. Turner, M.A. Fineman, R.F. Stebbings, J. Chem. Phys. 42 (1965) 4088.
[38] A. Henglein, K. Lacmann, G. Jacobs, Ber. Bunsenges. Phys. Chem. 63 (1965) 279.
[39] Z. Herman, J.D. Kerstetter, T.L. Rose, R. Wolfgang, Discuss. Faraday Soc. 44 (1967) 123.
[40] Z. Herman, J.H. Futrell, B. Friedrich, Int. J. Mass Spectrom. Ion Processes 58 (1984) 181.
[41] J. Kubišta, Z. Dolejšek, Z. Herman, Eur. Mass Spectrom. 4 (1998) 311.
[42] A.K. Shukla, S.G. Anderson, S.L. Howard, K.W. Sohlberg, J.H. Futrell, Int. J. Mass Spectrom. Ion Processes 86 (1988) 61.
[43] D.R. Herschbach, Discuss. Faraday Soc. 33 (1962) 149.
[44] B. Friedrich, Z. Herman, Collect. Czech. Chem. Commun. 49 (1984) 570.
[45] R. Wolfgang, R.J. Cross, J. Phys. Chem. 73 (1969) 743.
[46] F. Schneider, U. Havemann, L. Zülicke, V. Pacák, K. Birkinshaw, Z. Herman, Chem. Phys. Lett. 37 (1976) 323.
[47] M. Chiang, E.A. Gislason, B.H. Mahan, C.W. Tsao, A.S. Werner, J. Chem. Phys. 52 (1970) 2698.
[48] Z. Herman, J. Kerstetter, T.L. Rose, R. Wolfgang, Discuss. Faraday Soc. 44 (1967) 123.
[49] M. Sadílek, Z. Herman, J. Phys. Chem. 97 (1993) 2147.
[50] J. Zabka, Z. Dolejšek, J. Hrušák, Z. Herman, Int. J. Mass Spectrom. 185–187 (1999) 195.
[51] Z. Herman, M. Henchman, B. Friedrich, J. Chem. Phys. 93 (1990) 4916.
[52] J. Zabka, O. Dutuit, Z. Dolejšek, J. Polách, Z. Herman, Phys. Chem. Chem. Phys. 2 (2000) 781.
[53] M. Schweitzer, Thesis, University of Freiburg, 1993.
[54] D. Gerlich, U. Nowotny, Ch. Schlier, E. Teloy, Chem. Phys. 47 (1980) 245.
[55] M.A. Carpenter, J.M. Farrar, J. Phys. Chem. 101 (1997) 6870.
[56] Z. Herman, Int. Rev. Phys. Chem. 15 (1996) 299.
[57] Z. Herman, Phys. Essays 13 (2001) 480.
[58] S.D. Price, M. Manning, S.R. Leone, J. Am. Chem. Soc. 114 (1994) 8673.
[59] Z. Dolejšek, M. Fárník, Z. Herman, Chem. Phys. Lett. 235 (1995) 99.
[60] Z. Herman, J. Zabka, Z. Dolejšek, M. Fárník, Int. J. Mass Spectrom. 192 (1999) 191.
[61] P. M. Hierl, V. Pacák, Z. Herman, J. Chem. Phys. 67 (1977) 2678.
[62] Z. Herman, K. Birkinshaw, V. Pacak, Int. J. Mass Spectrom. Ion Processes 135 (1994) 47.
[63] J.H. Futrell, in Advances in Chemical Physics (State-Selected and State-to-State Ion-Molecule Reaction Dynamics: Experiment), C.Y. Ng, M. Baer (Eds.), Wiley, New York, 1992, Vol. LXXXII, p. 523.
[64] K. Birkinshaw, A. Shukla, S. Howard, J.H. Futrell, Chem. Phys. 113 (1987) 149.
[65] M. Noll, J.P. Toennies, J. Chem. Phys. 85 (1986) 3313.
[66] J. Los, Ber. Bunsenges. Phys. Chem. 77 (1973) 640.
[67] Collision Spectroscopy, R.G. Cooks (Ed.), Plenum Press, New York, 1978.
[68] J.A. Laramee, D.M. Hemberger, R.G. Cooks, J. Am. Chem. Soc. 91 (1979) 5202.
[69] J.A. Laramee, J.J. Carmody, R.G. Cooks, Int. J. Mass Spectrom. Ion Phys. 31 (1979) 333.
[70] Z. Herman, J.H. Futrell, B. Friedrich, Int. J. Mass Spectrom. Ion Processes 58 (1984) 181.
[71] K. Qian, A. Shukla, J.H. Futrell, J. Chem. Phys. 92 (1990) 5988.
[72] K. Qian, A. Shukla, J.H. Futrell, Rapid Commun. Mass Spectrom. 4 (1990) 222.
[73] R.E. Tosh, A.K. Shukla, J.H. Futrell, J. Phys. Chem. 99 (1995) 15488.
[74] A.K. Shukla, J.H. Futrell, J. Mass Spectrom. 35 (2000) 1069.
[75] F. Muntean, P.B. Armentrout, J. Chem. Phys. 115 (2001) 1213.